Mechanistic Studies of the 1,4-Polymerization of Butadiene According to the π-Allyl-Insertion Mechanism. 2. Density Functional Study of the C−C Bond Formation Reaction in Cationic and Neutral (η³-Crotyl)(η²-/η⁴-butadiene)nickel(II) Complexes [Ni(C₄H₇)(C₄H₆)]⁺, [Ni(C₄H₇)(C₄H₆)L]⁺ (L = C₂H₄, PH₃), and [Ni(C₄H₇)(C₄H₆)X] (X⁻ = I⁻)

Sven Tobisch,*,†,‡ Horst Bögel,† and Rudolf Taube*,§

*Institut für Physikalische Chemie der Martin-Luther-Universität Halle-Wittenberg,
Fachbereich Chemie (Merseburg), D-06099 Halle, Germany, and Anorganisch-Chemisches
Institut der Technischen Universität München, Lichtenbergstrasse 4,
D-85747 Garching, Germany*

The entire catalytic cycle of the 1,4-polymerization of butadiene has been theoretically studied according to the π-allyl-insertion mechanism. This has been performed using density functional theory (DFT) with cationic butenylbis(ligand) and neutral dimeric butenyl complexes as the catalyst. The calculations give a clear insight into the kinetic and thermodynamic control of the catalytic activity and cis−trans selectivity as well as into the elucidation of the stereoregulation mechanism. The supposed π-allyl-insertion mechanism was supported in all essential features by this research. The stability and reactivity of different isomers of η⁴-butadiene π-complexes was calculated to be very similar, regardless of the donor−acceptor ability of the neutral or anionic ligand. The thermodynamically more stable *syn*-butenyl forms are also more reactive than the anti counterparts. The intrinsic reactivity diminishes while the ligand's donating ability increases. The favored pathway proceeds in an exothermic process as follows: starting from stable *syn*-butenyl η⁴-*cis*-butadiene complexes, followed by a required ligand conversion via prone butadiene transition states, and subsequently anti−syn isomerization of the actual anti insertion product to a new transoid C₄ unit in the polymer chain. The polymer chain should not have any stereoselectivity in the methylene groups. Alternative pathways (e.g., via *anti*-butenyl prone butadiene transition states, thus forming a *cis*-1,4 polymer, or the direct generation of *trans*-1,4-products by inserting *trans*-butadiene) are strongly unfavored by higher kinetic barriers. The rate-determining step is the *cis*-butadiene insertion for the neutral complexes and the anti−syn isomerization for the cationic complexes. To achieve a well-balanced description of both thermodynamic and kinetic control of *trans*-1,4-polymerization of butadiene, a careful modeling of the organophosphorus ligand's basicity was necessary.

Introduction

To date, the stereoselective polymerization of mono-olefins and dienes using organometallic catalysts of the Ziegler−Natta-type[1] is highly likely, technically the most important catalytic reaction.[2] The *cis*-1,4-isomer has quickly gained much industrial importance among all of the different stereoisomers of polybutadiene, especially in tire production due to its natural rubber-like properties.

Several theoretical investigations at different computational levels have been performed to explain and understand the main process of ethylene polymerization,[3] the olefin insertion into a metal−alkyl bond. To

† Martin-Luther-Universität Halle-Wittenberg.
‡ E-mail: tobisch@chemie.uni-halle.de.
§ Technische Universität München.
(1) (a) Ziegler, K. *Angew. Chem.* **1964**, *76*, 545. (b) Natta, G. *Angew. Chem.* **1964**, *76*, 553.
(2) (a) *Applied Homogeneous Catalysis with Organometallic Complexes*; Cornils, B., Herrmann, W. A., Eds.; VCH: Weinheim, Germany, 1996. (b) Porri, L.; Giarrusso, A. In *Comprehensive Polymer Science*; Eastmond, G. C., Ledwith, A., Russo, S., Sigwalt, B., Eds.; Pergamon: Oxford, 1989; Vol. 4, Part II, pp 53−108.

(3) (a) Fuijimoto, H.; Yamasaki, T.; Mizutani, H.; Koga, N. *J. Am. Chem. Soc.* **1985**, *107*, 6157. (b) Kawamura-Kuribayashi, H.; Koga, N.; Morokuma, K. *J. Am. Chem. Soc.* **1992**, *114*, 2359. (c) Kawamura-Kuribayashi, H.; Koga, N.; Morokuma, K. *J. Am. Chem. Soc.* **1992**, *114*, 8687. (d) Koga, N.; Yoshida, T.; Morokuma, K. *Organometallics* **1993**, *12*, 2777. (e) Siegbahn, P. E. M. *Chem. Phys. Lett.* **1993**, *205*, 290. (f) Weiss, H.; Ehrig, M.; Ahlrichs, R. *J. Am. Chem. Soc.* **1994**, *116*, 4919. (g) Bierwagen, E. P.; Bercaw, J. E.; Goddard, W. A., III *J. Am. Chem. Soc.* **1994**, *116*, 1481. (h) Woo, T. K.; Fan, L.; Ziegler, T. *Organometallics* **1994**, *13*, 432. (i) Woo, T. K.; Fan, L.; Ziegler, T. *Organometallics* **1994**, *13*, 2252. (j) Fan, L.; Harrison, D.; Woo, T. K.; Ziegler, T. *Organometallics* **1995**, *14*, 2018. (k) Jensen, V. R.; Børve, K. J.; Ystenes, M. *J. Am. Chem. Soc.* **1995**, *117*, 4109. (l) Jensen, V. R.; Siegbahn, P. E. M. *Chem. Phys. Lett.* **1993**, *212*, 353. (m) Lohrenz, J. C. W.; Woo, T. K.; Fan, L.; Ziegler, T. *J. Organomet. Chem.* **1995**, *497*, 91. (n) Lohrenz, J. C. W.; Woo, T. K.; Ziegler, T. *J. Am. Chem. Soc.* **1995**, *117*, 12793

date, except for our previous investigation,[4] no theoretical study by means of reliable nonempirical methods has been carried out concerning the key step of the butadiene polymerization, the generation of new C_4 units in the growing chain by insertion of butadiene into the allyl-transition-metal bond.

In contrast to the rather simple ethylene insertion into a metal−alkyl bond, the elucidation of the mechanism of stereoregulation of butadiene polymerization proved to be a much more complicated task. Difficulties arose from the large number of different possibilities in the structure and reactivity of the polybutadienyl group and the catalytically active transition-metal complex. Therefore, four different modes of butadiene coordination (η^2-cis, η^4-cis, η^2-trans, η^4-trans) and two different structures of the η^3-coordinated butenyl end group (anti-η^3, syn-η^3) have to be taken into account, giving rise to eight structurally different catalyst complexes. All of these catalyst complexes, which may be in equilibrium, are capable of achieving the insertion step.

There are extensive and systematic investigations of the reactivity and cis−trans selectivity of four different types of (η^3-allyl)nickel(II) complexes for the allylnickel-catalyzed butadiene polymerization. These can be regarded as structurally well-defined "single site" catalyst complexes: (a) dimeric allylnickel(II) compounds $[C_3H_5NiX]_2$ ($X^- = Cl^-$, Br^-, I^-,[5a] $CF_3CO_2^-$ [5b]); (b) cationic allylbis(ligand)nickel(II) complexes $[C_3H_5NiL_2]PF_6$ (L = $P(OR)_3$,[5c] other ligands[5d]); (c) cationic C_8-allyl(monoligand)nickel(II) complexes $[NiC_8H_{13}L]PF_6$ (L = PPh_3 and other ligands[5e]); (d) cationic "ligand free" C_{12}-allylnickel(II) complexes $[NiC_{12}H_{19}]X$ ($X^- = B(C_6H_3$-$(CF_3)_2)_4^-$, PF_6^-, SbF_6^-, BF_4^-, and other ligands[5f–h]).

Two different mechanisms for the insertion of butadiene into to the allyl−transition-metal bond are proposed. Cossee and Arlman[6] first suggested that the η^2- or η^4-coordinated butadiene could be nucleophilically attacked by the butenyl end group in its η^1-coordination. In contrast to this σ-allyl-insertion mechanism, the butenyl group may also react with butadiene in its η^3-state, i.e., both reacting moieties are in π-coordination. This π-allyl-insertion mechanism was introduced by Taube et al.[7] The cis−trans selectivity according to this

mechanism is not determined by the rate of the anti−syn isomerization, as suggested in the literature,[8] but by the different reactivity of the *anti*- and *syn*-butenyl-nickel(II) complexes with respect to the mode of butadiene coordination. It can be concluded from the principle of least-structure variation that, in the 1,4-polymerization, the insertion of butadiene in the single cis configuration must lead to an anti structure of the new butenyl end group (anti insertion), whereas butadiene coordinated in the single trans configuration always indicates a syn structure (syn insertion). Moreover, the anti or syn configuration of the butenyl chain end group determines the cis or trans configuration of the double bond in the newly formed C_4 unit. When related to the cis−trans selectivity in the complex-catalyzed 1,4-polymerization of 1,3-dienes, this anti−cis and syn−trans correlation is now generally accepted as a fundamental feature of the mechanism.[2b]

In a previous paper[4a] on the C−C bond-formation reaction in cationic (η^3-allyl)(η^2/η^4-butadiene)nickel(II) complexes $[Ni(C_3H_5)(C_4H_6)]^+$ and $[Ni(C_3H_5)(C_4H_6)$-$(C_2H_4)]^+$, we were able to establish that the insertion of *cis*-butadiene into the allylnickel(II) bond can take place within the π-coordination of the reacting parts.

In this paper, we will present the results for the butadiene insertion into the (η^3-butenyl)nickel(II) bond in both cationic and neutral butenyl(monoligand)nickel(II) complexes. Starting with typical experimentally verified trans catalysts,[7e] i.e., dimeric allylnickel(II) $[Ni(\eta^3-C_3H_5)X]_2$ ($X^- = I$[5a]) and cationic allylbis(ligand)-nickel(II) $[Ni(\eta^3-C_3H_5)L_2]X$ (L = $P(OPh)_3$,[5c] PPh_3[5d]) complexes, respectively, *trans*-1,4-polymer units should be formed via *cis*-butadiene insertion into the *syn*-(η^3-butenyl)nickel(II) bond in cationic and neutral butenyl(monoligand)nickel(II) complexes. The proposed catalytic reaction mechanism of the *trans*-1,4-polymerization of butadiene (according to k_{1t}) with cationic butenylbis-(ligand)nickel(II) complexes is depicted in Scheme 1. The catalytic cycle for neutral butenyl(monoligand)nickel(II) complexes differ from Scheme 1 in the starting dimeric (η^3-allyl)nickel(II) complex, **1**, and the corresponding dimeric butenyl complexes, **2**. Scheme 1 also contains the competitive pathway of forming *cis*-1,4-polymer units (according to k_{1c}) by walking through the branch, which is initiated by *cis*-butadiene insertion into the *anti*-(η^3-butenyl)nickel(II) bond. The essential steps of the catalytic cycle have been elucidated by ^{31}P NMR spectroscopy for the bis(triphenyl phosphite) complex $[Ni(\eta^3-C_3H_5)(P(OPh)_3)_2]PF_6$.[7a]

Starting with (η^3-allyl)bis(ligand)nickel(II) or dimeric (η^3-allyl)nickel(II) complexes **1**, the corresponding butenyl complexes **2** are formed after a short initialization period, which can be regarded as stable store complexes under polymerization conditions. Subsequently, two kinds of butenyl(monoligand)(butadiene)nickel(II) complexes are formed by successive neutral- or anionic-ligand substitution, which differ in the mode of butadiene coordination i.e., η^2, **3**, or η^4, **4**. To accomplish the required C(1)−C(1) connection of the reactive butadiene and butenyl moieties (which, in π-coordination, occupy the two opposite coordination sites in the metal

(4) (a) Tobisch, S.; Bögel, H.; Taube, R. *Organometallics* **1996**, *15*, 3563. (b) Bögel, H.; Tobisch, S. *Int. J. Quantum Chem., Quantum Chem. Symp.* **1996**, *30*, 197.

(5) (a) Lazutkin, A. M.; Vashkevich, V. A.; Medvedvev, S. S.; Vasiliev, V. N. *Dokl. Akad. Nauk* **1967**, *175*, 859. (b) Hadjiandeou, P.; Julemont, M.; Teyssie, P. *Macromolecules* **1984**, *17*, 2455. (c) Taube, R.; Schmidt, U.; Gehrke, J.-P.; Anacker, U. *J. Prakt. Chem.* **1984**, *326*, 1. (d) Taube, R.; Gehrke, J.-P.; Schmidt, U. *J. Organomet. Chem.* **1985**, *292*, 287. (e) Taube, R.; Gehrke, J.-P.; Böhme, P.; Köttnitz, J. *J. Organomet. Chem.* **1990**, *395*, 341. (f) Taube, R.; Böhme, P.; Gehrke, J.-P *J. Organomet. Chem.* **1990**, *399*, 327. (g) Taube, R.; Langlotz, J. *Macromol. Chem.* **1993**, *194*, 705. (h) Wache, S.; Taube, R. *J. Organomet. Chem.* **1993**, *456*, 137.

(6) (a) Cossee, P. In *Stereochemistry of Macromolecules*; Ketley A. D., Ed.; Marcel Dekker Inc.: New York, 1967; Vol. 1, p 145. (b) Arlman, E. J. *J. Catal.* **1966**, *5*, 178.

(7) (a) Taube, R.; Gehrke, J.-P.; Radeglia, R. *J. Organomet. Chem.* **1985**, *291*, 101. (b) Taube, R.; Gehrke, J.-P.; Böhme, P. *Wiss. Z. Tech. Hochsch. Leuna-Merseburg* **1987**, *39*, 310. (c) Sieler, J.; Kempe R.; Wache, S.; Taube, R. *J. Organomet. Chem.* **1993**, *455*, 241. (d) Taube, R.; Wache, S.; Sieler, J.; Kempe, R. *J. Organomet. Chem.* **1993**, *456*, 131. (e) Taube, R.; Schmidt, U.; Gehrke, J.-P.; Böhme, P.; Langlotz, J.; Wache, S. *Makromol. Chem., Macromol. Symp.* **1993**, *66*, 245. (f) Taube, R.; Windisch, H.; Maiwald, S. *Makromol. Chem., Macromol. Symp.* **1995**, *89*, 393. (g) Taube, R.; Sylvester, G. In *Applied Homogeneous Catalysis with Organometallic Complexes*; Cornils, B., Herrmann, W. A., Eds.; VCH: Weinheim, Germany, 1996; pp 280−317.

(8) (a) Jolly, P. W.; Wilke, G. The Organic Chemistry of Nickel. Organic Synthesis, Academic Press: New York, 1975; Vol. 2, p 225. (b) Dolgoplosk, B. A. *Sov. Sci. Rev., Sect. B* **1980**, *2*, 203.

Scheme 1. Catalytic Cycle of the 1,4-Polymerization of Butadiene with Cationic Butenylbis(ligand) Complexes [Ni(η^3-RC$_3$H$_4$)L$_2$]$^+$ as the Catalyst
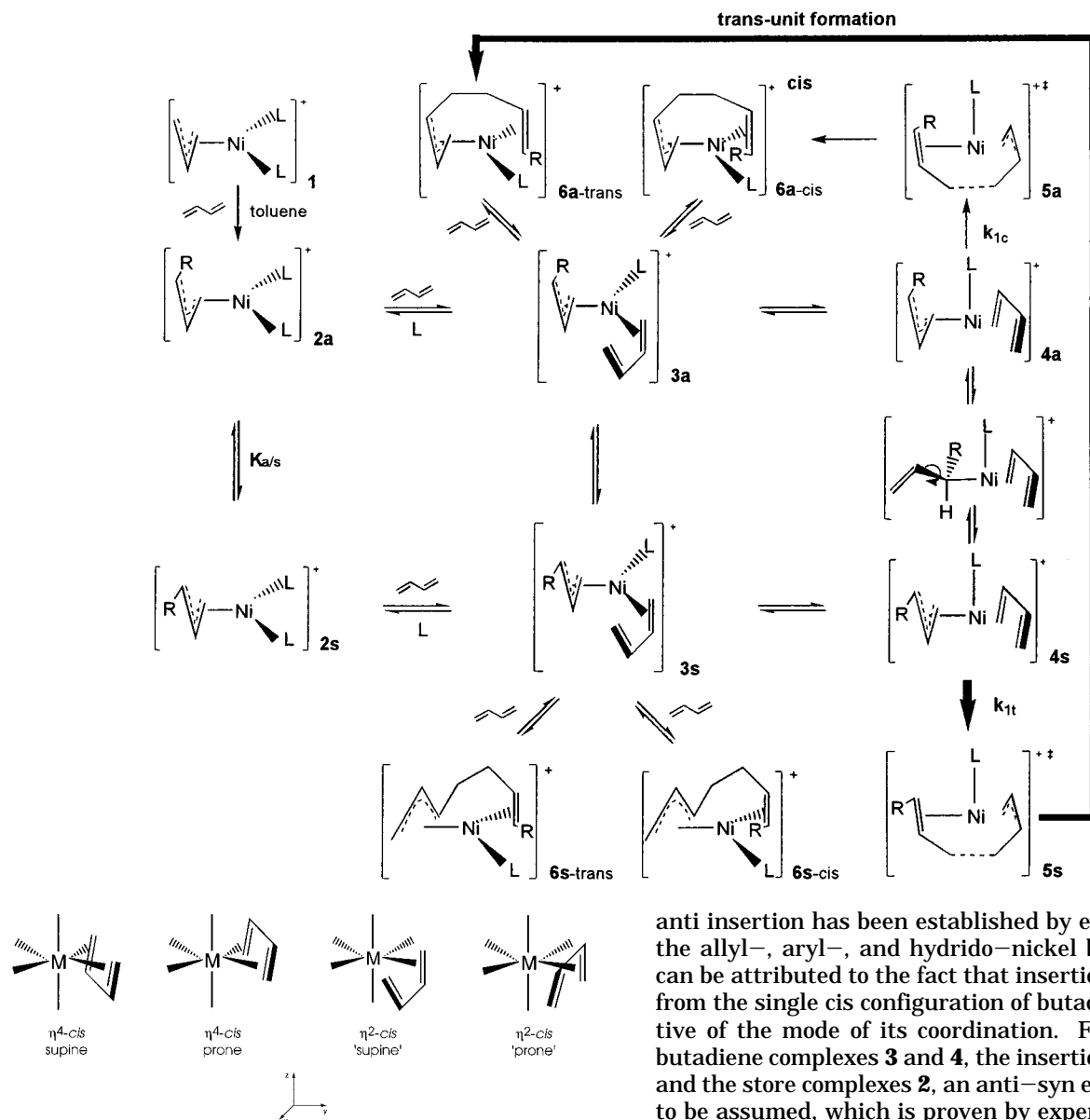

Figure 1. Structurally different modes of *cis*-butadiene coordination at the metal M in the butadiene π-complexes.

coordination plane), two different orientations of *cis*-butadiene, i.e., supine and prone,[9] are possible when dealing with both modes of coordination (cf. Figure 1). Depending on the donor–acceptor ability of the neutral ligand L or the anionic ligand X, respectively, the most reactive form of either the η^2- or η^4-butadiene π-complexes should represent the actual catalyst complex. *cis*-Butadiene insertion takes place through transition states **5**, that lead to the insertion products **6a**; in turn, the polymer chain is elongated by a new C$_4$ unit containing one new double bond. Simultaneously, an η^3-coordinated butenyl group in the anti configuration is regenerated as the chain end from the butadiene, thus allowing the polymerization to proceed. This should be possible if the next butadiene is capable of replacing the last π-coordinated double bond of the growing polymer chain in order to form a new η^4-butadiene complex. The

anti insertion has been established by experiments for the allyl–, aryl–, and hydrido–nickel bond.[7a,10] This can be attributed to the fact that insertion starts solely from the single cis configuration of butadiene, irrespective of the mode of its coordination. For each of the butadiene complexes **3** and **4**, the insertion products **6a**, and the store complexes **2**, an anti–syn equilibrium has to be assumed, which is proven by experiment[7a] in the case of **2**. This is indicated by $K_{a/s}$ in Scheme 1 and schematically depicted by a supposed σ-Ni–C(3) structure lying between the syn and anti forms of the η^4-butadiene complexes **4a** and **4s**. Within this paper, different forms of the complexes are labeled with an **s** and **a** for the syn and anti configurations of the butenyl group, respectively. In the course of generating *trans*-1,4-polymer units by anti insertion, the products **6a** (which always give rise to a cis *anti*-butenyl configuration at the reactive end) have to undergo anti–syn isomerization.

The objective of this research is to apply density functional theory to shed light on the mechanistic aspects of the stereoselective polymerization of butadiene according to the proposed π-allyl-insertion mechanism. To this end, competitive reaction pathways for butadiene insertion into the *anti/syn*-(η^3-butenyl)nickel(II) bond are investigated. This provides insight on

(9) Yasuda, H.; Nakamura A. *Angew. Chem.* **1987**, *99*, 745.

(10) (a) Lehmkuhl, H.; Keil, T.; Benn, R.; Rufinska, A.; Krüger, C.; Poplawska, J.; Bellenbaum, M. *Chem. Ber.* **1988**, *121*, 1931. (b) Tolman, C. A. *J. Am. Chem. Soc.* **1970**, *92*, 6777.

the differences in reactivity between the anti- and *syn*-butenyl(monoligand)(butadiene)nickel(II) complexes, the key feature which determines the cis−trans selectivity. By comparing the reactivity of the different mutual orientations of the reacting parts, we expect to find some evidence that will elucidate the stereoregulation mechanism. It is interesting to see how the nature of the neutral or anionic ligand influences the intrinsic reactivity and the cis−trans selectivity of the insertion process, as well as the position of the substitution equilibrium between the store complex, **2**, and the real catalyst complexes, **3** or **4**. Furthermore, the conditions required to open the trans channel will be examined. Finally, the course of the anti−syn isomerization will be explored in detail, to determine which of the two successive processes, insertion or isomerization, is the rate-determining step. However, any alternative competing mechanism, i.e., the σ-allyl-insertion mechanism, shall not be investigated. We believe that a symbiotic fusion of high-level quantum-chemical calculations together with experiments provides a real chance in finding solutions to solve these and other related mechanistic problems.

Computational Details

The approximate density functional calculations reported here were performed by using the DGauss program within the UniChem software environment.[11]

All calculations were carried out using the LDA with Slater's exchange functional[12a,b] and Vosko−Wilk−Nusair parametrization on the homogeneous electron gas for correlation,[12c] augmented by gradient corrections to the exchange-correlation potential. Gradient corrections for exchange based on the functional of Becke[12d] and for correlation based on Perdew[12e] were added variationally within the SCF procedure (LDA/BP-NLSCF).

All electron Gaussian orbital basis sets were used for all atoms. The calculations were performed with a standard DZVP basis which consists of a 15s/9p/5d set contracted to (63321/531/41) for nickel,[13a] a 9s/5p/1d set contracted to (621/41/1) for carbon,[13b] and a 4s/1p set contracted to (31/1) for hydrogen.[13b] The corresponding auxiliary basis sets were used for fitting the charge density.[13b]

For all of the calculations, the fine integration grid option was used. The effect of tighter-meshed grids (xfine grid option) was evaluated to be not more than 0.2 kcal/mol for total energies, as indicated by single-point calculations with more than twice as many integration points as our standard fine grid.

The geometry optimization and the saddle-point search were performed at the LDA/BP-NLSCF level of approximation by utilizing analytical gradients/Hessians according to standard algorithms. No symmetry constraints were imposed in any optimization. The stationary points were identified exactly by the curvature of the potential-enery surface at these points corresponding to the eigenvalues of the analytically calculated Hessian. The zero-point energy correction (ZPC) and Gibbs free-energy calculations (at 298 K and 1 atm) were performed

for the reactants, transition states, and products, which describes the full catalytic cycle for the cationic $[Ni(C_4H_7)(C_4H_6)L]^+$ (L = PH_3, PF_3, PMe_3, $P(OMe)_3$) and the neutral $[Ni(C_4H_7)(C_4H_6)X]$ ($X^- = I^-$) model systems.

The intrinsic energy of inserting s-cis butadiene into a C−C bond, thus forming a *cis*-1,4-polymer chain (the energy gain from breaking one C−C double bond and forming a C−C single bond during the insertion), without a catalytically active Ni(II) center was estimated as the average value of the exothermicities which were obtained for the general reaction $C_4H_7\text{-}(C_4H_6)_n\text{-}C_4H_7 + C_4H_6 \rightarrow C_4H_7\text{-}(C_4H_6)_{n+1}\text{-}C_4H_7$ ($n = 0-2$). It amounts to 22.0 and 18.5 kcal/mol (without and with ZPC, respectively), which is in excellent agreement with the experimental value of 18.7 kcal/mol (determined if the polymerization proceeds in the gas phase[14]).

Results and Discussion

Here, the results obtained from our DFT calculations on the cationic $[Ni(C_4H_7)(C_4H_6)(C_2H_4)]^+$ and $[Ni(C_4H_7)(C_4H_6)PH_3]^+$ and the neutral $[Ni(C_4H_7)(C_4H_6)I]$ complexes, which were chosen as minimal models of the real active catalyst, the butenyl(monoligand)(butadiene)-nickel(II) complexes $[RC_3H_4Ni(C_4H_6)L]^+$ and $[RC_3H_4Ni(C_4H_6)X]$, shall be presented. In each of the model systems, both the *anti*- and *syn*-crotyl forms and four different butadiene complexes have been investigated, which originate from the prone and the opposite supine[9] orientation of each of the reacting crotyl and butadiene moieties (thus giving rise to supine/supine, *SS*, supine/prone, *SP*, prone/supine, *PS*, and prone/prone, *PP*; where in XY, X and Y are related to crotyl and butadiene, respectively). In addition, two different modes of butadiene coordination (η^2-cis and η^4-cis) were taken into account giving rise to sixteen competitive butadiene complexes. In the case of the quasi-planar 16-electron complexes **2** and **6**, however, the *SS* and *PP* and the *SP* and *PS* orientations are identical concerning the coordination pattern. Although the anti insertion of butadiene, which means that butadiene must insert from the s-cis configuration, has been thoroughly proven by experiment,[7a,10] additionally the η^2-trans and η^4-trans modes of butadiene coordination have been examined for the $[Ni(C_4H_7)(C_4H_6)PH_3]^+$ and $[Ni(C_4H_7)(C_4H_6)I]$ systems. To get an idea about the reliability of modeling real *trans*-1,4-selective catalyst systems, e.g., where L = PPh_3, $P(OPh)_3$, by using the computationally less-demanding, simplified PH_3 ligand, this research was extended to L = PMe_3, $P(OMe)_3$, PF_3. Additionally, for comparison with our previous investigation[4a] on the $[Ni(C_3H_5)(C_4H_6)]^+$ complex, the $[Ni(C_4H_7)(C_4H_6)]^+$ system was examined. The effect of the counterion or solvent in the catalytic process was neglected considering the present computational resources available. Moreover, the influence of a solvent should not be of primary concern since this type of polymerization occurs in noncoordinating aromatic hydrocarbons such as toluene or benzene.

With respect to our previous research,[4a] it is now possible to differentiate the reactivity and stability of *anti*- and *syn*-butadiene complexes. In addition, the effect of the different modeling of the real butenyl group by going from allyl to crotyl is examined. It would be interesting to see whether an additional neutral or

(11) (a) Andzelm, J.; Wimmer, E. *Physica B* **1991**, *172*, 307. (b) Andzelm, J. In *Density Functional Methods in Chemistry*; Labanowski, J., Andzelm, J., Eds.; Springer: Berlin, 1991. DGauss and UniChem are software packages available from Cray Research.

(12) (a) Dirac, P. A. M. *Proc. Cambridge Philos. Soc.* **1930**, *26*, 376. (b) Slater, J. C. *Phys. Rev.* **1951**, *81*, 385. (c) Vosko, S. H.; Wilk, L.; Nusair, M. *Can. J. Phys.* **1980**, *58*, 1200. (d) Becke, A. D. *Phys. Rev.* **1988**, *A38*, 3098. (e) Perdew, J. P. *Phys. Rev.* **1986**, *B33*, 8822.

(13) (a) DGauss basis set library. (b) Godbout, N.; Salahub, D. R.; Andzelm, J.; Wimmer, E. *Can. J. Chem.* **1992**, *70*, 560.

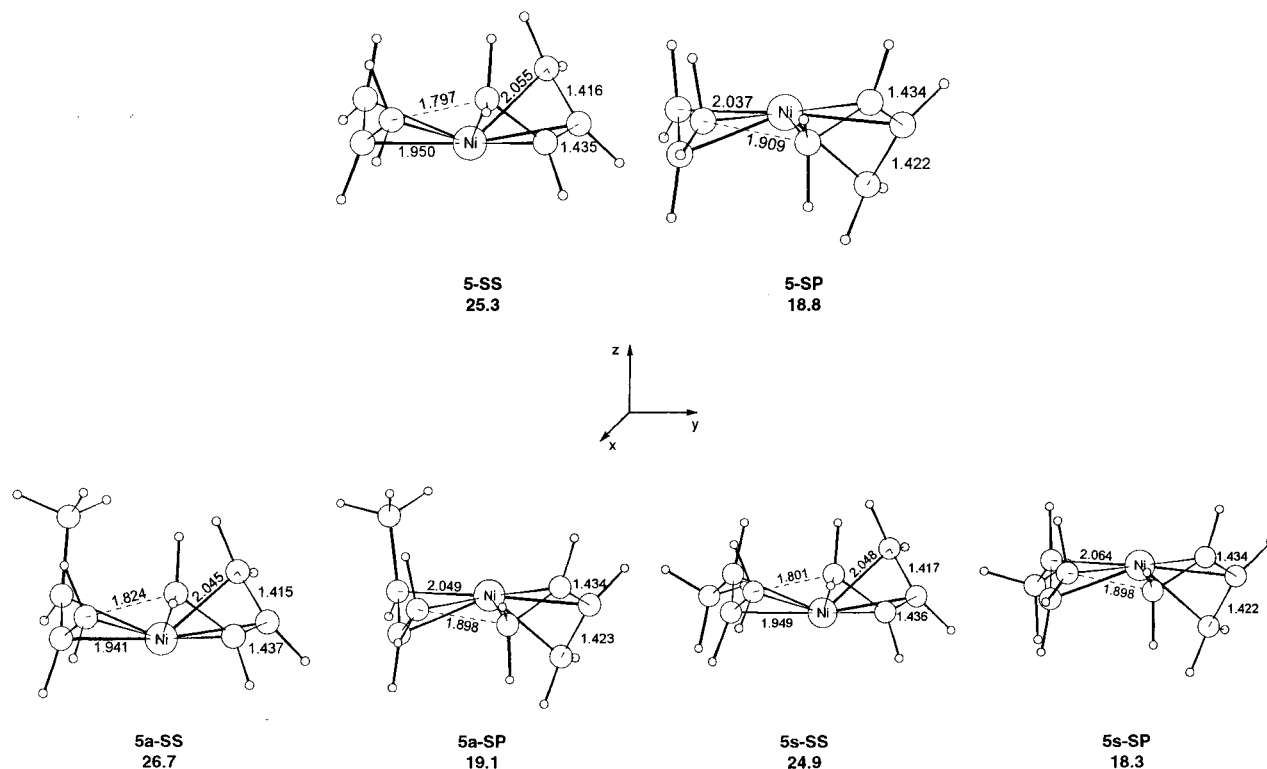(14) Robert, D. E. *J. Res. Natl. Bur. Stand.* **1950**, *44*, 221.

Figure 2. Selected geometrical parameters of the optimized structures (Å) of the transition states for *cis*-butadiene insertion into $[Ni(C_3H_5)(C_4H_6)]^+$ (top) and $[Ni(C_4H_7)(C_4H_6)]^+$ (bottom) together with the activation energies (ΔE in kcal/mol) relative to **4**-*SS* and **4s**-*SS*, respectively.

anionic ligand, instead of the coordinated double bond from the growing polymer chain, is able to make the insertion process energetically practical. Of special interest is how the nature of the ligand, i.e., neutral ligands (C_2H_4, PH_3) versus anionic ligands (I^-) or strong σ-donor ligands (I^-, PH_3) versus π-donor/acceptor ligands (C_2H_4), may influence the stability and reactivity of the butadiene complexes. The need for an additional ligand is expected to be found in order to obtain reliable energetics of the insertion process, in compliance with our previous research.[4a] The kind of butadiene coordination (η^2- or η^4-) which is preferred in the process of forming stable π-complexes should be determined by the ligand's donating abilities.

We will start with the investigation of the π-allyl insertion on the above-mentioned model systems. Attention will be focused primarily on the energetic aspects of the insertion process, because the main geometrical features and the important orbital interactions responsible for the different stability and reactivity of different butadiene π-complexes are examined in detail in our previous study,[4a] performed on the prototype 16/14 electron $[Ni(C_3H_5)(C_4H_6)]^+$ and 18/16 electron $[Ni(C_3H_5)(C_4H_6)(C_2H_4)]^+$ systems. These systems were recalculated in the present study in order to get a consistent picture, since minor changes in the computational procedure appear when compared with the former one. The first step toward our objective of theoretically studying the entire catalytic cycle of *trans*-1,4-polymerization will be to start to explore the insertion cycle **3/4** → **5** → **6a** → **3/4** (cf. Scheme 1). After analyzing the major features that determine the polymerization by kinetic control, the discussion will be followed by an examination of the position of the ligand substitution equilibrium between **2** and **3** or **4**, respec-

tively. This should give insight into the thermodynamic control of the polymerization. Moreover, the anti−syn isomerization will be investigated. Finally, the Gibbs free-energy profile calculated for the entire reaction cycle of the *trans*-1,4-polymerization of butadiene is given.

We start with $[Ni(C_4H_7)(C_4H_6)]^+$, as compared with $[Ni(C_3H_5)(C_4H_6)]^+$, and continue with a detailed examination of the ligand influence in $[Ni(C_4H_7)(C_4H_6)L]^+$ and $[Ni(C_4H_7)(C_4H_6)X]$.

Cationic $[Ni(C_3H_5)(C_4H_6)]^+$ and $[Ni(C_4H_7)(C_4H_6)]^+$ Complexes. The variations in geometry of the allyl-nickel−butadiene framework of η^2-, η^4-butadiene π-complexes, **3** and **4**, transition states, **5**, and insertion products, **6a**, are negligible for the *syn*- and *anti*-crotyl complexes compared with the allyl complexes for both the *SS* and *SP* arrangement, respectively, as well as between the *SS* and *SP* orientations. Selected geometrical parameters of the optimized transition-state structures are shown in Figure 2. No clear influence of *anti*/*syn*-crotyl versus allyl is apparent from the optimized geometries, and therefore, the major orbital interaction and the stability and activity of the corresponding structures of both types of complexes are expected to be nearly identical.

In the first step, *cis*-butadiene binds to the metal d[8] center forming stable butadiene π-complexes in an η^4-mode, **4**, which is preferred to the η^2-mode, **3**, because the coordination number is increased. Whereas in **4** butadiene formally occupies two sites opposite to the allyl/crotyl moiety in the square-planar Ni(II) coordination plane (assumed to be the *xy* plane), in **3** only one coordination site is occupied, thus butadiene appears as vinylethene. The *SP* orientation is favored due to the energy of the *SS* orientation, which may be at-

Table 1. Calculated Potential Energy Profiles for the *cis*-Butadiene Insertion into the Cationic $[Ni(C_3H_5)(C_4H_6)]^+$ (I) and $[Ni(C_4H_7)(C_4H_6)]^+$ (II) Complexes (kcal/mol)[a]

system	4 BE[b]	4	3	5 $\Delta E^{\ddagger c}$	5 $\Delta E^{\ddagger}_{abs}{}^d$	6a ΔE^e
			$[Ni(C_3H_5)(C_4H_6)]^+$ (I)			
SS	−68.7	0.0	19.7	25.3	25.3	8.6
SP	−71.1	−2.4	20.4	21.2	18.8	3.8
			$[Ni(C_4H_7)(C_4H_6)]^+$ (II)			
anti-SS	−62.8	2.1	19.0	24.6	26.7	7.1
anti-SP	−66.0	−1.1	20.0	20.2	19.1	4.5
syn-SS	−64.9	0.0	16.7	24.9	24.9	8.9
syn-SP	−67.0	−2.1	17.5	20.4	18.3	4.3

[a] **4**-*SS* (**I**), **4s**-*SS* (**II**) was chosen as the reference point. [b] The stabilization energy of **4** relative to the isolated reactants ($[Ni(\eta^3\text{-}C_3H_5/C_4H_7)]^+$ and *s-cis*-C_4H_6). [c] The activation energy relative to the corresponding isomer of **4**. [d] The activation energy relative to **4**-*SS* (**I**), **4s**-*SS* (**II**). [e] The reaction energy relative to the corresponding isomer of **4**.

tributed to the subtle interplay of bonding and antibonding interactions of the formally vacant d_{xy} Ni(II) orbital with the HOMO's of the allyl/crotyl and butadiene. A detailed discussion of this topic is given in our previous paper.[4a]

In the second step, *cis*-butadiene inserts into the butenylnickel(II) bond via the transition states, **5**, forming the insertion products, **6a**. The product structures are already preformed in the transition states, and the process of forming the new C−C σ-bond can be clearly observed, while the reacting parts still retain π-coordination. The transition states are characterized by an almost complete change in the hybridization of the affected carbon atoms of the newly formed C−C σ-bond from sp² to sp³. This was explained in detail in our previous study.[4a]

The energy profiles for the $[Ni(C_3H_5)(C_4H_6)]^+$ and $[Ni(C_4H_7)(C_4H_6)]^+$ systems are reported in Table 1. As indicated by minor changes in the geometry, no obvious influence of the butenyl group in its anti or syn configuration to the stability and reactivity of the butadiene complexes can be observed, as compared with the $[Ni(C_3H_5)(C_4H_6)]^+$ system. Only small differences may be detected between the *SS* and *SP* orientations.

The overall reaction starting from the isolated fragments is strongly exothermic, but the insertion reaction (relative to **4**) was calculated to be endothermic by about 8 and 4 kcal/mol for the *SS* and *SP* orientations, respectively. The formation of η^4-butadiene complexes is favored by about 21 kcal/mol (for the most reactive *SP* forms) relative to the η^2-mode. For the insertion step to occur, the η^2-π-complexes should only be transient forms during the process of forming η^4-butadiene complexes, in accordance with the principle of least-structure variation. Concerning **4**, the *SP* orientation is about 2−3 kcal/mol more stable than *SS* and the syn form is approximately 2 and 1 kcal/mol more stable than the anti form for *SS* and *SP*, respectively, in accordance with the experimental results. Quite large activation barriers of approximately 25 and 20 kcal/mol were obtained for *SS* and *SP*, respectively. In contrast to our previous study,[4a] the thermodynamically more stable *SP* η^4-butadiene complexes are also favored by kinetic control. Due to nearly identical absolute insertion barriers for the most reactive *anti-* and *syn-SP* forms of **4**, the reactivity amounts to be comparable for both

butenyl group configurations. It should give rise to a equibinary polymerization product, in contrast to experimental findings, i.e., no cis−trans selectivity can be derived from these simple model systems.

As a general result, no obvious effect of the butenyl group's configuration, regardless of whether the butenyl group was modeled by crotyl or allyl, on the geometric, electronic, and energetic features of the insertion process was apparent for the simple cationic $[Ni(C_3H_5)(C_4H_6)]^+$ and $[Ni(C_4H_7)(C_4H_6)]^+$ model systems. The differences in the stability and activity of butadiene complexes are slightly more pronounced if the mutual orientation of butenyl and butadiene is changed. Therefore, these simple model systems are unable to reliably describe the energetic features of the insertion process. In addition, a closer inspection of the cis−trans selectivity does not seem to be very meaningful.

Cationic $[Ni(C_3H_5)(C_4H_6)(C_2H_4)]^+$, $[Ni(C_4H_7)(C_4H_6)L]^+$ (L = C_2H_4, PH_3), and $[Ni(C_4H_7)(C_4H_6)X]$ ($X^- = I^-$) Complexes. As described in detail in our previous paper,[4a] the coordination of an additional ligand gives rise to a fundamental change in the geometric, electronic, and energetic features of the insertion process. Assuming that allyl/crotyl and butadiene are π-coordinated to nickel within the *xy* plane via interaction of their HOMO's with the formally vacant metal d_{xy} orbital, two different kinds of coordination of the reactive butenyl and butadiene moieties can be distinguished in **5** (cf. Figure 3). This is caused by an additional ligand, which is coordinated in an axial *z*-position. Butadiene coordination in a supine mode, i.e., *SS* and *PS* orientations, gives rise to a quadratic pyramid (spread out by the terminal carbons of the allylic and butadiene moieties and the additional ligand above this plane). On the other hand, butadiene coordination in a prone mode, i.e., *SP* and *PP* orientations, gives rise to a trigonal bipyramid (spread out by the terminal allylic carbons, the butadiene C(1) carbon, which forms the new C−C bond, and the additional ligand and the butadiene C(4) carbon above and below to this triangular plane). The stability may be deduced from the different extent of interaction of the HOMO of allyl/crotyl and butadiene with the appropriate metal d orbitals. An explanation of the orbital interactions in the different ligand orientations is given in detail in our previous study.[4a]

The key structures describing the insertion process, the butadiene π-complexes **3** and **4**, the transition states **5**, and the insertion products **6a**, exhibit similar geometrical features regardless of the additional ligand's nature. Figure 3 shows the geometries of the optimized transition-state structures together with relevant structural data for all of the different ligand orientations in the case of the cationic $[Ni(C_3H_5)(C_4H_6)(C_2H_4)]^+$ and $[Ni(C_4H_7)(C_4H_6)(C_2H_4)]^+$ complexes. However, only the most stable transition-state structures are illustrated in Figure 4 for the cationic (with L = PH_3) and neutral complexes (with $X^- = I^-$).

In the transition states the ligand has to move from its axial position toward an equatorial position, which may depend on the degree of rehybridization of the affected carbons of the newly formed C−C σ-bond from sp² to sp³. Therefore, these carbons will move away from the Ni(II) coordination sphere. Due to the effective
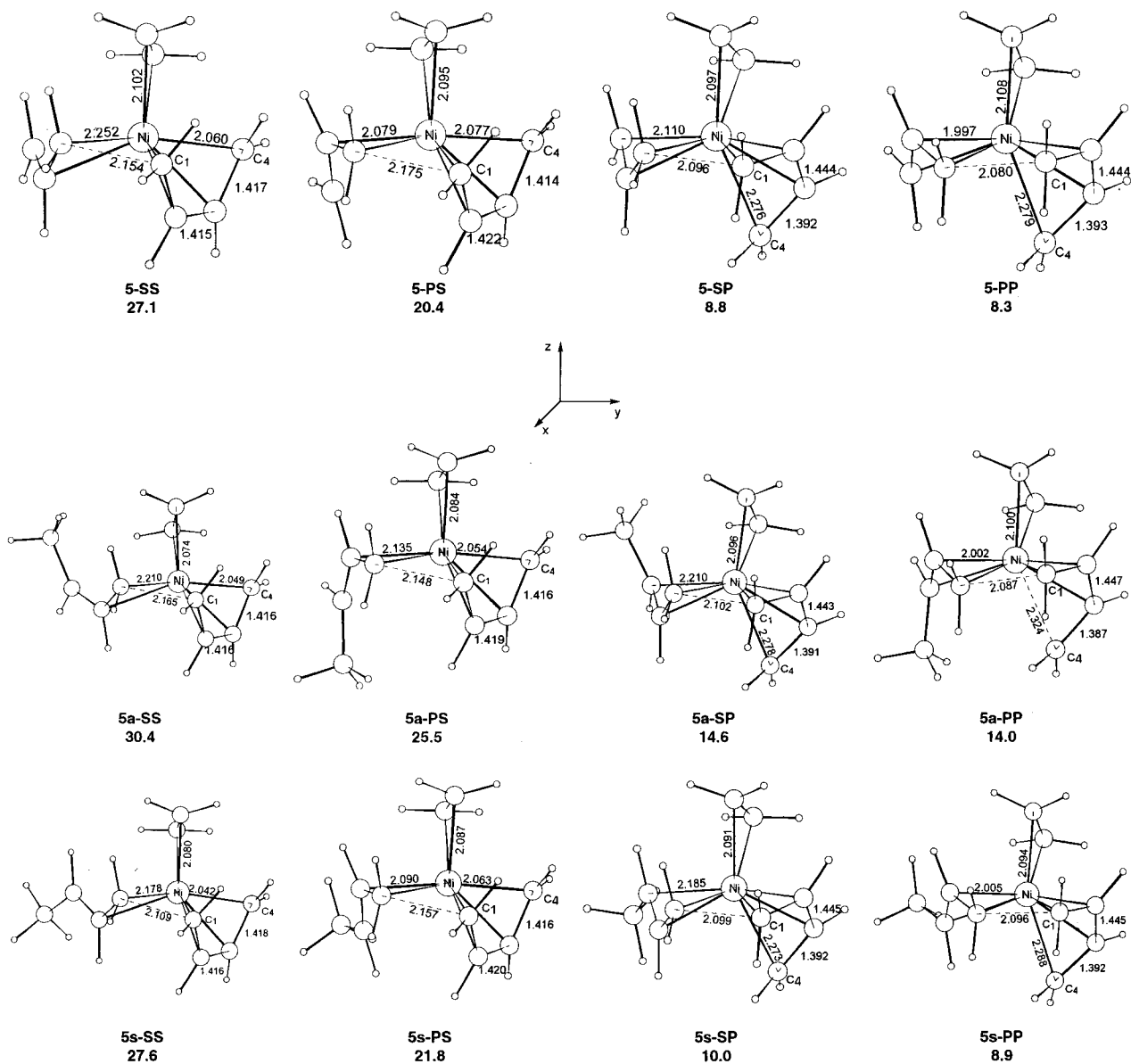
Figure 3. Selected geometrical parameters of the optimized structures (Å) of the transition states for *cis*-butadiene insertion into $[Ni(C_3H_5)(C_4H_6)(C_2H_4)]^+$ (top) and $[Ni(C_4H_7)(C_4H_6)(C_2H_4)]^+$ (bottom) together with the activation energies (ΔE in kcal/mol) relative to **4**-*SS* and **4s**-*SS*, respectively.

interaction of prone butadiene with the d_{z^2} nickel AO, it should be easier for prone butadiene to reach the transition state than for supine butadiene, which yields a significantly reduced activation barrier. Additionally, the *SP* and *PP* isomers of **5** appear educt-like, whereas the geometry of the *SS* and *PS* transition states is, on the whole, determined by the insertion products, **6a**. In contrast to the preceding complexes (without a ligand that may formally occupy the fifth coordination place), now the *SS* orientation is the most stable isomer of **4**, as experimentally found for several kinds of complexes.[15] This may be attributed to the fact that in this orientation butenyl and butadiene are better able to avoid the repulsive interaction with the axial ligand (by slightly moving from the coordination plane as com-

pared with the other orientations) by simultaneously retaining a strong bonding interaction in the quasi-planar coordination plane.

The energetics calculated for the $[Ni(C_3H_5)(C_4H_6)\text{-}(C_2H_4)]^+$, $[Ni(C_4H_7)(C_4H_6)(C_2H_4)]^+$ and $[Ni(C_4H_7)(C_4H_6)\text{-}(PH_3)]^+$, $[Ni(C_4H_7)(C_4H_6)I]$ complexes are reported in Tables 2 and 3, respectively. As compared with the preceding systems, Tolman's 18–16-electron rule was fulfilled by an additional ligand and, therefore, the insertion amounts to be strongly exothermic by about 15–25 kcal/mol, with the corresponding butadiene π-complexes (**4**) chosen as reference. Moreover, the energetic gap between the η^4- and η^2-butadiene complexes is significantly reduced. Concerning the process of forming stable π-complexes, butadiene preferably coordinates in an η^4-mode and the most stable η^2-complex lies a few kcal/mol higher in energy, which depends on the ligand. The differences in the stability of the butadiene complexes are not significantly influenced by ZPC and contributions caused by thermal

(15) (a) Harlow, R. L.; Krusic, P. J.; McKinney, R. J.; Wreford, S. S. *Organometallics* **1982**, *1*, 1506. (b) Yasuda, H.; Tatsumi, K.; Okamoto, T.; Mashima, K.; Lee, K.; Nakamura, A.; Kai, Y.; Kaneshisa, N.; Kasai, N. *J. Am. Chem. Soc.* **1985**, *107*, 2410. (c) Okamoto, T.; Yasuda, H.; Nakamura, A.; Kai, Y.; Kaneshisa, N.; Kasai, N. *Organometallics* **1988**, *7*, 2266.
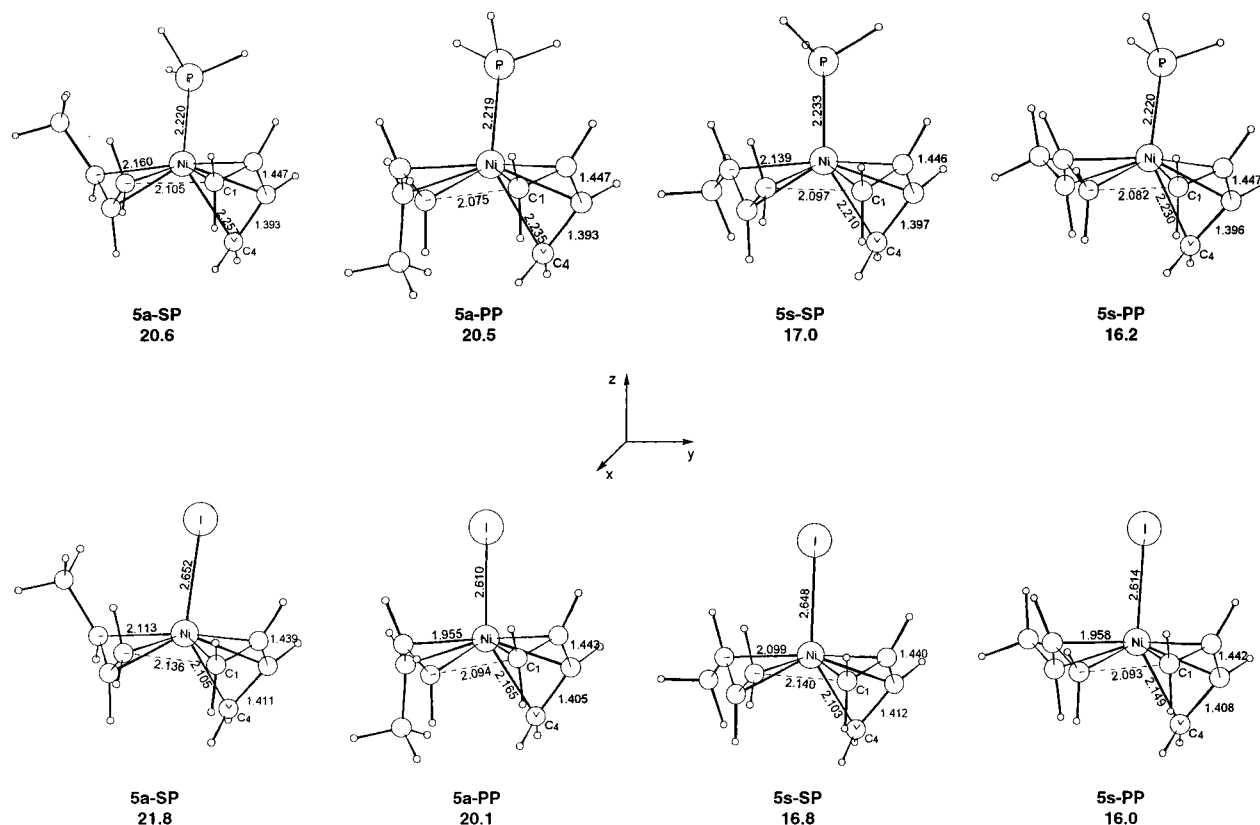
Figure 4. Selected geometrical parameters of the optimized structures (Å) of the most stable transition states for *cis*-butadiene insertion into $[Ni(C_4H_7)(C_4H_6)PH_3]^+$ (top) and $[Ni(C_4H_7)(C_4H_6)I]$ (bottom) together with the activation energies (ΔE in kcal/mol) relative to **4s**-*SS*.

Table 2. Calculated Potential-Energy Profiles for the *cis*-Butadiene Insertion into the Cationic $[Ni(C_3H_5)(C_4H_6)(C_2H_4)]^+$ (I) and $[Ni(C_4H_7)(C_4H_6)(C_2H_4)]^+$ (II) Complexes (kcal/mol)[a]

system	**4** BE^b	**4**	**3**	**5** $\Delta E^{\ddagger\,c}$	**5** $\Delta E^{\ddagger}{}_{abs}{}^d$	**6a** ΔE^e
	$[Ni(C_3H_5)(C_4H_6)(C_2H_4)]^+$ (I)					
SS	−37.0	0.0	4.4	27.1	27.1	−11.0
PS	−36.1	0.9	4.1	19.5	20.4	−14.8
SP	−33.8	3.2	4.1	5.6	8.8	−17.1
PP	−32.1	4.9	4.4	3.4	8.3	−15.9
	$[Ni(C_4H_7)(C_4H_6)(C_2H_4)]^+$ (II)					
anti-SS	−29.8	3.7	7.4	26.7	30.4	−10.6
anti-PS	−28.9	5.6	8.3	19.9	25.5	−16.6
anti-SP	−25.5	9.0	8.3	5.6	14.6	−20.0
anti-PP	−23.4	11.1	7.4	2.9	14.0	−18.0
syn-SS	−33.2	0.0	6.4	27.6	27.6	−7.5
syn-PS	−30.7	1.9	6.0	19.9	21.8	−12.6
syn-SP	−29.7	4.8	6.0	5.2	10.0	−15.4
syn-PP	−27.8	6.7	6.4	2.2	8.9	−14.2

[a] **4**-*SS* (I), **4s**-*SS* (II) was chosen as the reference point. [b] The stabilization energy of **4** relative to the isolated reactants ($[Ni(\eta^3\text{-}C_3H_5/C_4H_7)(\eta^2\text{-}C_2H_4)]^+$ and *s-cis*-C_4H_6). [c] The activation energy relative to the corresponding isomer of **4**. [d] The activation energy relative to **4**-*SS* (I), **4s**-*SS* (II). [e] The reaction energy relative to the corresponding isomer of **4**.

motion. The most stable η^4-butadiene complexes stem from supine butadiene (with *SS* as the most stable orientation), which are by approximately 3−4 kcal/mol more stable than the prone butadiene forms, independent of the additional ligand. The energetic effect is less pronounced if the butenyl orientation changes from supine to prone, approximately 1 and 2 kcal/mol (ΔE) for the $[Ni(C_3H_5)(C_4H_6)(C_2H_4)]^+$ and $[Ni(C_4H_7)(C_4H_6)(C_2H_4)]^+$ systems, respectively. The different orienta-

tions also have a minor influence on the stability of the isomers of **3**. The stability of the butadiene complexes is mainly determined by the kind of butadiene orientation, and the energetic influence of an additional methyl group is rather small when going from allyl to crotyl. As compared with the $[Ni(C_4H_7)(C_4H_6)]^+$ system, the interaction of the butenyl group with the axial ligand in **4** gives rise to an increased anti−syn gap of about 4 kcal/mol (ΔE, in favor of the syn form), which is less pronounced in **3** but is preserved in **5**, regardless of the ligand's nature.

Similar to the stability of butadiene complexes, there is no apparent influence of crotyl compared with allyl on the intrinsic reactivity in the case of $[Ni(C_3H_5)(C_4H_6)(C_2H_4)]^+$ and $[Ni(C_4H_7)(C_4H_6)(C_2H_4)]^+$ systems. Independent of the ligand's nature, starting from the most stable isomers of **4**, the insertion process is strongly disabled by large activation barriers, especially for the most stable *SS* orientation, of about 20−30 kcal/mol (ΔE). These barriers are roughly identical to those calculated for the $[Ni(C_3H_5)(C_4H_6)]^+$ and $[Ni(C_4H_7)(C_4H_6)]^+$ systems. On the other hand, however, the insertion barrier becomes significantly decreased for the prone butadiene coordination, f.i., for the ethylene ligand the barrier is decreased to approximately 6 and 3 kcal/mol with ZPC (7 and 4 kcal/mol using the Gibbs free energy) for *SP* and *PP*, respectively. This may indicate that the insertion is quite feasible for these orientations. Thus, the less stable prone butadiene isomers of **4** are most reactive. Therefore, a ligand conversion, which is supposed to proceed with no kinetic barrier, has to take place for the η^4-butadiene complexes

Table 3. Calculated Potential-Energy (with and without ZPC) and Gibbs Free-Energy Profile for the *cis*-Butadiene Insertion into the Cationic [Ni(C₄H₇)(C₄H₆)(PH₃)]⁺ (I) and the Neutral [Ni(C₄H₇)(C₄H₆)I] (II) Complexes (kcal/mol)[a]

system	4 BE[b]	4	3	5 $\Delta E^{\ddagger}$ [c]	5 $\Delta E^{\ddagger}_{abs}$ [d]	6a ΔE [e]
			[Ni(C₄H₇)(C₄H₆)(PH₃)]⁺ **(I)**			
anti-SS	−40.4	2.8 (2.8)	10.1 (9.2)	29.5 (29.7)	32.3 (32.5)	−7.9 (−6.0)
		2.9	*6.8*	*29.5*	*32.4*	*−6.1*
anti-PS	−36.3	7.0 (7.1)	9.9 (9.0)	22.5 (22.3)	29.5 (29.4)	−15.4 (−13.9)
		6.9	*7.8*	*22.3*	*29.2*	*−13.9*
anti-SP	−30.6	12.6 (12.4)	9.9 (9.0)	8.0 (8.3)	20.6 (20.7)	−21.0 (−19.2)
		11.6	*7.8*	*9.6*	*21.2*	*−18.6*
anti-PP	−26.7	16.5 (16.2)	10.1 (9.2)	4.0 (4.4)	20.5 (20.6)	−21.6 (−19.4)
		15.3	*6.8*	*5.2*	*20.5*	*−18.5*
syn-SS	−43.3	0.0 (0.0)	9.1 (8.2)	28.3 (28.2)	28.3 (28.2)	−5.4 (−3.5)
		0.0	*7.1*	*28.4*	*28.4*	*−3.8*
syn-PS	−40.1	3.2 (2.9)	8.5 (7.6)	22.8 (23.0)	26.0 (25.9)	−12.2 (−10.4)
		2.1	*6.4*	*23.7*	*25.8*	*−9.3*
syn-SP	−33.3	9.8 (8.9)	8.5 (7.6)	7.1 (7.0)	17.0 (16.5)	−18.9 (−17.0)
		8.7	*6.4*	*7.4*	*16.0*	*−15.8*
syn-PP	−31.1	12.1 (11.5)	9.1 (8.2)	4.1 (4.5)	16.2 (16.0)	−17.5 (−15.0)
		10.7	*7.1*	*5.0*	*15.7*	*−14.5*
			[Ni(C₄H₇)(C₄H₆)I] **(II)**			
anti-SS	−18.3	3.1 (2.9)	3.2 (2.6)	28.9 (28.8)	32.0 (31.7)	−11.3 (−9.3)
		2.7	*1.2*	*28.8*	*31.5*	*−9.2*
anti-PS	−14.3	7.1 (7.0)	3.2 (2.5)	21.9 (21.8)	29.0 (28.8)	−20.9 (−18.8)
		4.5	*1.0*	*24.8*	*29.3*	*−16.2*
anti-SP	−9.4	12.0 (11.9)	3.2 (2.5)	9.8 (10.2)	21.8 (22.1)	−25.8 (−23.7)
		11.1	*1.0*	*11.6*	*22.7*	*−22.8*
anti-PP	−8.0	13.4 (13.3)	3.2 (2.6)	6.7 (7.0)	20.1 (20.3)	−21.6 (−19.7)
		12.6	*1.2*	*8.2*	*20.8*	*−19.1*
syn-SS	−21.4	0.0 (0.0)	1.9 (1.2)	26.8 (26.6)	26.8 (26.6)	−8.6 (−6.6)
		0.0	*−0.4*	*26.8*	*26.8*	*−6.5*
syn-PS	−18.2	3.2 (2.9)	1.7 (1.1)	21.8 (21.8)	25.0 (24.7)	−17.5 (−15.2)
		2.5	*−0.3*	*22.0*	*24.5*	*−14.3*
syn-SP	−13.6	7.8 (7.5)	1.7 (1.1)	9.0 (9.4)	16.8 (16.9)	−22.1 (−19.8)
		6.9	*−0.3*	*10.4*	*17.3*	*−18.7*
syn-PP	−11.4	10.0 (9.8)	1.9 (1.2)	6.0 (6.4)	16.0 (16.2)	−18.6 (−16.4)
		9.3	*−0.4*	*7.3*	*16.6*	*−15.8*

[a] **4s**-*SS* was chosen as the reference point; numbers in parentheses include the zero-point correction while those in italics are the Gibbs free energies. [b] The stabilization energy of **4** relative to the isolated reactants ([Ni(*syn*-η³-C₄H₇)PH₃/I]⁽⁺⁾ and *s-cis* C₄H₆). [c] The activation energy relative to the corresponding isomer of **4**. [d] The activation energy relative to **4s**-*SS*. [e] The reaction energy relative to the corresponding isomer of **4**.

from *SS* to *PP* to carry out the insertion at the favorable pathway. The conversion process needs about 7, 10, and 12 kcal/mol with ZPC for C₂H₄, I⁻, and PH₃, which is quite similar to or somewhat larger than the energetic gap between the **4**-*SS* and **3**-*SP/PP* complexes for the neutral or the anionic ligands, respectively. Therefore, η⁴- together with η²-butadiene complexes should be in comparable concentration in the educt equilibrium. However, the transition states of the insertion must be formed via the η⁴-*cis*-butadiene complexes, as deduced from the principle of least-structure variation. The η²-complexes, however, can be regarded as being possible, but transient π-complexes in the course of butadiene insertion are followed by η⁴-butadiene complex formation.

For the given ligand, the intrinsic reactivity ($\Delta E^{\ddagger}$) of prone butadiene complexes is nearly identical for the anti- and *syn*-crotyl forms. The cis−trans selectivity is determined by the absolute barrier heights ($\Delta E^{\ddagger}_{abs}$) of the most reactive anti and syn complexes, i.e., relative to the most stable *syn*-η⁴-butadiene complex, **4s**-*SS*. The strong trans selectivity of the 1,4-polymerization of butadiene for cationic [Ni(C₄H₇)(C₄H₆)L]⁺ and neutral [Ni(C₄H₇)(C₄H₆)X] system is obvious from the calculated $\Delta E^{\ddagger}_{abs}$ values reported in Tables 2 and 3. Therefore, the thermodynamically more stable *syn*-butenyl forms are also more reactive than the corresponding *anti*-

butenyl counterparts. In addition, the minor difference in the stability of the transition states of the most reactive *syn*-butenyl complexes is remarkable, regardless of whether the butenyl group is coordinated supine or prone. With the assumption of a prepared *syn-SP* to *syn-PP* equilibrium, which is supposed to be sufficiently rapid under the given conditions, it may be deduced that for the *trans*-1,4 butadiene polymerization no stereoselectivity can be expected within the methylene groups of the growing polymer chain, as found by experiment.[16]

Now the competitive reaction pathway of *trans*-butadiene insertion will be discussed for the cationic [Ni(C₄H₇)(C₄H₆)PH₃]⁺ and neutral [Ni(C₄H₇)(C₄H₆)I] systems, which leads to a straight route to a *trans*-1,4 polymer (cf. Scheme 1, the *syn*-butenyl *trans*-butadiene insertion product **6s**-*trans*) without anti−syn isomerization, as required for the *cis*-butadiene insertion. Attention is focused only on the examination of the transition states because of their absolute stability, as compared with the most stable transition states for the *cis*-butadiene insertion. This will indicate whether the insertion along this reaction pathway is likely or unlikely to occur with regard to the *cis*-butadiene

(16) (a) Porri, L.; Aglietto, M. *Macromol. Chem.* **1976**, *177*, 1465. (b) Stephenson, L. M.; Kovac, C. A. *ACS Symp. Ser.* **1983**, *212*, 307.
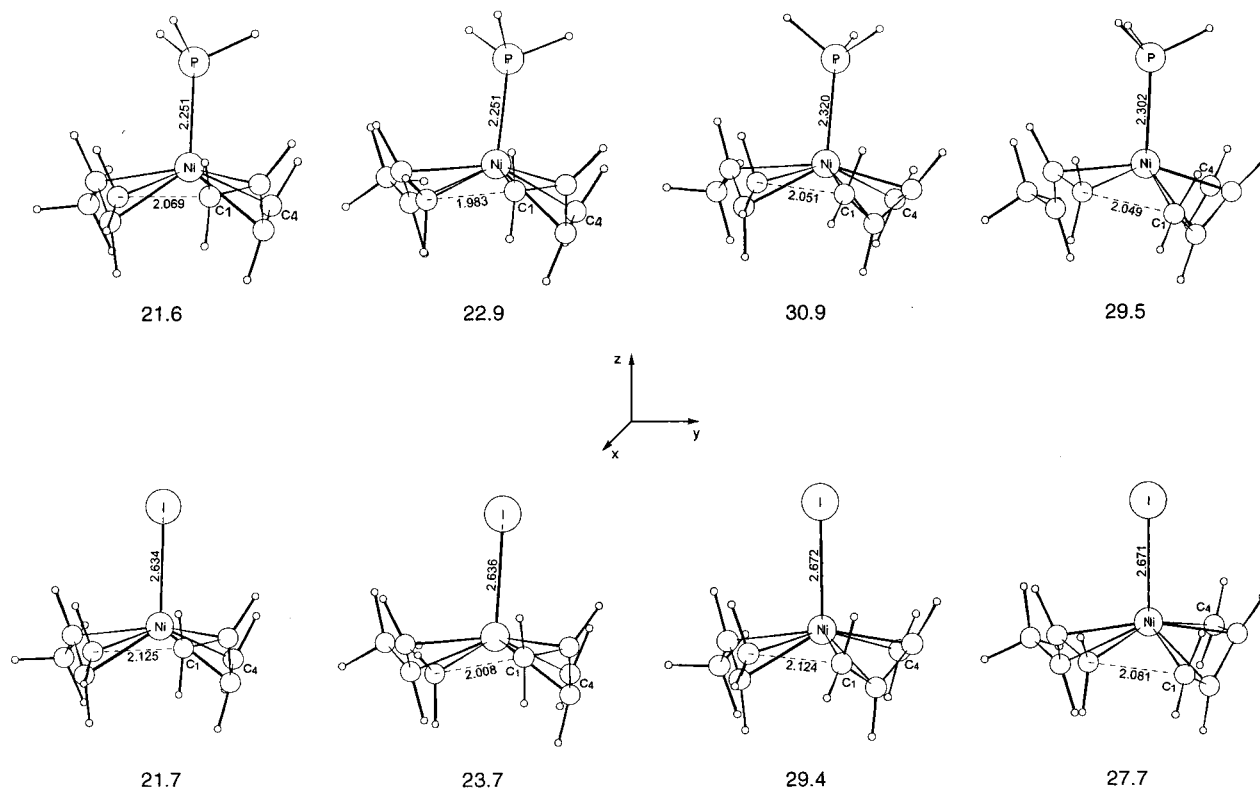
Figure 5. Selected geometrical parameters of the optimized structures (Å) of the transition states for *trans*-butadiene insertion into $[Ni(C_4H_7)(C_4H_6)PH_3]^+$ (top) and $[Ni(C_4H_7)(C_4H_6)I]$ (bottom) together with the activation energies (ΔE in kcal/mol) relative to **4s**-*SS*.
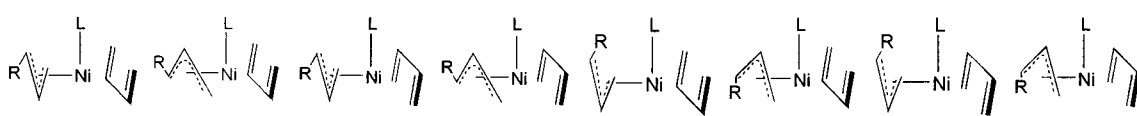
insertion. According to the *cis*-butadiene insertion, the *syn*-butenyl forms are more stable and, therefore, more reactive than the anti counterparts. The most stable *anti*-butenyl transition states are 4.1 and 4.5 kcal/mol with ZPC (5.1 and 4.8 kcal/mol using the Gibbs free energy), less stable than the most stable *syn*-butenyl transition state for PH_3 and I, respectively. Four possible *syn*-butenyl transition states, together with the activation energy relative to the most stable **4s**-*SS* complex, are shown in Figure 5. The favored transition state for *cis*-butadiene insertion is about 4.6 and 4.7 kcal/mol with ZPC (4.0 and 4.1 kcal/mol using the Gibbs free energy) more stable relative to the trans counterpart for the neutral and anionic model ligand, respectively. Therefore, it may be deduced that the butadiene insertion starting from the trans configuration is very unlikely, thus this reaction pathway should be insignificant in the course of the entire polymerization process. The distinct preference of butadiene insertion from the s-cis configuration is in agreement with the evidence for the anti insertion as found experimentally[7a,10] and supports the basic assumption of the proposed π-allyl-insertion mechanism.

To conclude, a neutral or anionic ligand, instead of the next coordinated double bond of the growing polymer chain as modeled by the ethylene ligand, should be able to make the insertion process of *cis*-butadiene into a (η^3-butenyl)nickel(II) bond quite practicable, with the reactive moieties in π-coordination. The insertion of *trans*-butadiene as a competitive reaction pathway is unlikely because of significantly higher insertion barriers as compared with the *cis*-butadiene insertion. Therefore, the reaction pathway via *trans*-butadiene insertion should be ruled out in the course of the entire

polymerization process. Furthermore, after the insertion product undergoes the necessary anti–syn isomerization, the insertion should take place starting from the thermodynamically more stable *syn*-butenyl complexes via prone butadiene transition states, leading to a *trans*-1,4-polymer chain elongated by a new C_4 unit. This is the preferred reaction pathway for cationic and neutral monoligand complexes.

Comparison of the Stability and Reactivity of η^4-Butadiene $[Ni(C_4H_7)(C_4H_6)L]$ (L = C_2H_4, PH_3) and $[Ni(C_4H_7)(C_4H_6)X]$ (X^- = I^-) Complexes. The stability and reactivity of the different isomers of butadiene complexes **4** are calculated to be very similar and quite comparable, regardless of the donor–acceptor ability of the neutral or the anionic ligand (cf. the summary reported in Table 4). In each case, the syn forms are more stable than the anti counterparts and η^4 coordination is preferred in general to η^2-butadiene coordination. The stability of the different isomers of **4** is mainly determined by the kind of butadiene orientation rather than by that of the butenyl group, which is less pronounced. The most stable isomers of **4** stem from the *syn-SS* coordination, whereas the most stable *syn-SP* η^2-butadiene complexes are disfavored by 1.7, 6.0, and 8.5 kcal/mol (ΔE) for I^-, C_2H_4, and PH_3, respectively. This gap decreases considerably by the stronger donating anionic ligand, since the η^2-coordination can compete better with the η^4-coordination with an increasing electron density on the metal center. The gap is reduced to −0.4 and 6.4 kcal/mol in the Gibbs free energy for I^- and PH_3.

Prone butadiene isomers of **4** are calculated to be much more reactive than the supine counterparts. For the most stable *SS* orientation, the insertion is almost

Table 4. Summary of Calculated Stability and Activity of η^4-Butadiene [Ni(C$_4$H$_7$)(C$_4$H$_6$)L/X]$^{(+)}$ Complexes (kcal/mol)^a

L / X$^-$	4s-SS	4s-PS	4s-SP	4s-PP	4a-SS	4a-PS	4a-SP	4a-PP
C$_2$H$_4$	0.0 (0.0)	1.9 (1.9)	4.8 (4.6)	6.7 (6.5)	3.7 (3.7)	5.6 (5.9)	9.0 (8.7)	11.1 (10.9)
	0.0	*1.7*	*4.8*	*6.2*	*3.8*	*6.1*	*7.4*	*11.3*
PH$_3$	0.0 (0.0)	3.2 (2.9)	9.9 (9.5)	12.1 (11.5)	2.8 (2.8)	7.0 (7.1)	12.6 (12.4)	16.5 (16.2)
	0.0	*2.1*	*8.6*	*10.7*	*2.9*	*6.9*	*11.6*	*15.3*
I$^-$	0.0 (0.0)	3.2 (2.9)	7.8 (7.5)	10.0 (9.8)	3.1 (2.9)	7.1 (7.0)	12.0 (11.9)	13.4 (13.3)
	0.0	*2.5*	*6.9*	*9.3*	*2.7*	*4.5*	*11.1*	*12.6*
$\Delta E^{\#b}$								
C$_2$H$_4$	27.6 (27.1)	19.9 (20.1)	5.2 (5.6)	2.2 (2.7)	26.7 (26.3)	19.9 (19.7)	5.6 (6.2)	2.9 (3.7)
	26.9	*21.0*	*6.1*	*3.7*	*25.5*	*19.8*	*8.4*	*4.1*
PH$_3$	28.3 (28.2)	22.8 (23.0)	7.1 (7.0)	4.1 (4.5)	29.5 (29.7)	22.5 (22.3)	8.0 (8.3)	4.0 (4.4)
	28.4	*23.7*	*7.4*	*5.0*	*29.5*	*22.3*	*9.6*	*5.2*
I$^-$	26.8 (26.6)	21.8 (21.8)	9.0 (9.4)	6.0 (6.4)	28.9 (28.8)	21.9 (21.8)	9.8 (10.2)	6.7 (7.0)
	26.8	*22.0*	*10.4*	*7.3*	*28.8*	*24.8*	*11.6*	*8.2*
$\Delta E^{\#}_{abs}{}^{c}$								
C$_2$H$_4$	27.6 (27.1)	21.8 (22.0)	10.0 (10.2)	8.9 (9.2)	30.4 (30.0)	25.5(25.6)	14.6 (14.9)	14.0 (14.6)
	26.9	*22.7*	*10.9*	*9.9*	*29.3*	*25.9*	*15.8*	*15.4*
PH$_3$	28.3 (28.2)	26.0 (25.9)	17.0 (16.5)	16.2 (16.0)	32.3 (32.5)	29.5 (29.4)	20.6 (20.7)	20.5 (20.6)
	28.4	*25.8*	*16.0*	*15.7*	*32.4*	*29.2*	*21.2*	*20.5*
I$^-$	26.8 (26.6)	25.0 (24.7)	16.8 (16.9)	16.0 (16.2)	32.0 (31.7)	29.0 (28.8)	21.8 (22.1)	20.1 (20.3)
	26.8	*24.5*	*17.3*	*16.6*	*31.5*	*29.3*	*22.7*	*20.8*

^{a} **4s**-*SS* was chosen as the reference point in each case; numbers in parentheses include the zero-point correction while those in italics are the Gibbs free energies. ^{b} The activation energy relative to the corresponding isomer of **4**. ^{c} The activation energy relative to **4s**-*SS*.

disabled by a rather large barrier and, therefore, the reactive butadiene and butenyl moieties must change their mutual orientation to open the favored pathway via prone butadiene transition states. The energy required to destabilize the most stable isomer toward the most reactive butadiene isomer of **4** is determined to a greater extent by butadiene rather than by butenyl group conversion. Although both kinds of butadiene complexes should be in comparable concentrations in the educt equilibrium, the η^2-butadiene π-complexes cannot be considered as the direct precursor of the transition states of the insertion process, while complying with the principle of least-structure variation. Rather, they could be regarded as transient forms during the process of forming the η^4-butadiene complexes on the way to the transition states.

Nearly identical activation barriers for *anti*- and *syn*-butenyl forms indicate a similar intrinsic reactivity (cf. $\Delta E^{\ddagger}$), regardless of the butenyl group's configuration. The intrinsic reactivity (relative to **4s**-*SS*) becomes diminished with the increasing ligand donating ability in the order C$_2$H$_4$ > PH$_3$ > I$^-$, as indicated by the activation barrier's growth (including ZPC) of each of about 2 kcal/mol in the order C$_2$H$_4$ (2.6 kcal/mol), PH$_3$ (4.5 kcal/mol), and I$^-$ (6.4 kcal/mol) for the most reactive butadiene complexes. Under purely kinetic control, *cis*-butadiene insertion would preferably proceed via *syn*-butenyl prone butadiene transition states, regardless of whether *SP* or *PP* orientations are concerned, thus opening the *trans*-1,4 reaction channel, which yields a polymer product that in turn does not possess any stereoselectivity in the methylene groups. Alternative pathways, i.e., via *anti*-butenyl prone butadiene transition states, forming a *cis*-1,4 polymer, or the direct generation of *trans*-1,4 products (without subsequent anti−syn isomerization) by inserting *trans*-butadiene, are strongly unfavored by higher kinetic barriers.

Thermodynamic Control of Polymerization. Until now, the course of the polymerization process was investigated only on purely kinetic grounds, which were based on calculated kinetic barriers of competitive pathways for butadiene insertion. This has been assumed to be the rate-determining step. Apart from the kinetic control, the catalytic activity is also determined by the concentration of the catalytically active butadiene complexes **4**, which are under polymerization conditions in a substitution equilibrium together with the stable store complexes **2**. Therefore, the activity observed experimentally, given in turnover numbers, consists, in any case, of a rate constant and an equilibrium constant.

The ligand or double-bond substitution by butadiene supposedly takes place without any significant kinetic barrier[17] (with Ni(II) in a spin-paired d^8 configuration), thus the substitution reaction can be regarded to be equilibrated. Under this assumption, it is only necessary to know the stability of both of the complexes, **2** and **4**, regardless of the transient system's stability that may be involved during the reaction **2** → **4**. The difference in the thermodynamic stability determines the position of the equilibrium and, therefore, the concentration of the active catalyst complex. All of the complexes, which are in a substitution equilibrium, may

(17) (a) *Mechanismen in der anorganischen Chemie*; Basolo, F., Pearson, R. G., Eds.; G. Thieme Verlag: Stuttgart, Germany, 1973. (b) *Comprehensive Coordination Chemistry*; Wilkinson, G., Gillard, R. D., McClevery, J. A., Eds.; Pergamon Press: New York, 1987; Vol. I, pp 281−384. (c) Cross, R. J. *Chem. Soc. Rev.* **1985**, *14*, 197. (d) Cross, R. J. *Adv. Inorg. Chem.* **1989**, *34*, 219.
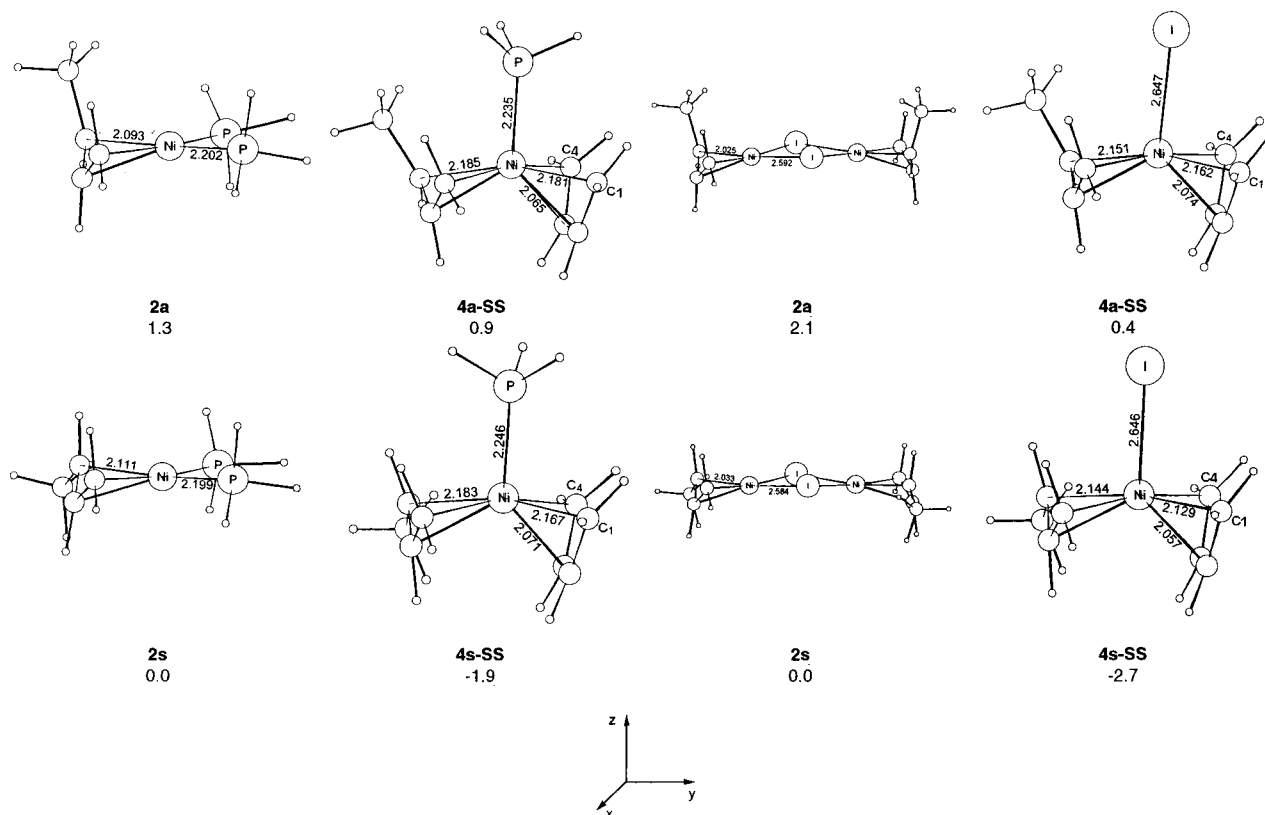
Figure 6. Selected geometrical parameters of the optimized structures (Å) of bis(ligand) $[Ni(C_4H_7)L_2]^+$ and η^4-butadiene $[Ni(C_4H_7)(C_4H_6)L]^+$ complexes (L = PH_3, right) and dimeric $[Ni(C_4H_7)X]_2$ and η^4-butadiene $[Ni(C_4H_7)(C_4H_6)X]$ complexes ($X^- = I^-$, left) together with the relative energies (ΔE in kcal/mol).

undergo anti–syn isomerization. The *syn*-butenyl forms are, in any case, thermodynamically more stable than the *anti*-butenyl counterparts.

The position of the substitution equilibrium between the stable store complexes, **2**, and the thermodynamically most stable isomers of the real catalyst complex, **4**-*SS*, is evaluated for the cationic and neutral complexes with L = PH_3 and $X^- = I^-$, respectively (cf. Figure 6). For the cationic complexes $[Ni(C_4H_7)(PH_3)_2]^+$, **2a** and **2s**, and $[Ni(C_4H_7)(C_4H_6)(PH_3)]^+$, **4a**-*SS* and **4s**-*SS*, the *anti*-butenyl forms are calculated to be 1.3 and 2.8 kcal/mol, with ZPC, less stable than the *syn*-counterparts, respectively. Furthermore, the bis(ligand) complexes, **2**, are 1.8 and 0.3 kcal/mol, with ZPC, less stable relative to the corresponding butadiene complexes, **4**-*SS*, respectively. This may indicate that the equilibrium position should be mainly on the side of the catalyst complex, in contrast to ^{31}P NMR spectroscopic measurements.[7a] It has been conclusively proven experimentally that the bis(ligand) complex is the stable store complex. Therefore, the substitution equilibrium must strongly lie on the side of the bis(ligand) complex. On the other hand, the calculations suggest (without of inclusion of the entropy contribution) that the real catalytically active butadiene complexes should be formed almost completely from the bis(ligand) complexes. Therefore, the activity of cationic butenylbis(ligand) complexes should be determined mainly by kinetic control. It is hard to believe that the thermodynamic control of the polymerization could be properly described by the calculations, bearing in mind the rather small insertion barrier height and the experimentally determined activities of typical catalyst complexes. In

our opinion, the main reason for the difficulties could arise from the insufficient description of real ligand's basicity, such as PPh_3 and $P(OPh)_3$, by the simplified PH_3 model. There are also steric reasons, since ligand substitution by butadiene could more easily be possible by increasing the ligand's bulkiness due to an increased steric hindrance in **2**. We believe the electronic reason to be superior. Therefore, the investigation will be extended to L = PMe_3, $P(OMe)_3$, and PF_3 for the thermodynamic control of the polymerization cycle in the case of the neutral ligands. Details will be given in a subsequent section. The substitution equilibrium position is shifted toward the bis(ligand) complexes, **2**, with inclusion of the entropy contribution, since complexes **2** are 1.6 and 3.4 kcal/mol more stable in the Gibbs free energy relative to the corresponding butadiene complexes, **4**-*SS*.

For the neutral complexes $[Ni(C_4H_7)I]_2$, **2a** and **2s**, and $[Ni(C_4H_7)(C_4H_6)I]$, **4a**-*SS* and **4s**-*SS*, the *anti*-butenyl forms are calculated to be 2.1 and 3.1 kcal/mol (ΔE) less stable than the syn counterparts, respectively. The bis(ligand) complexes, **2**, are 2.7 and 1.7 kcal/mol (ΔE) less stable relative to the corresponding butadiene complexes, **4**-*SS*, respectively. This difference in stability decreases after inclusion of ZPC to 0.7 and −0.4 kcal/mol, respectively. Thus, the substitution equilibrium is to nearly the same amount on both sides of the reaction **2** → **4**. Therefore, in contrast to the cationic complexes, the catalytically active butadiene complexes **4** should be detectable in the reaction solution. This has been proven by experiment.[19]

Anti–Syn Isomerization. Here, stable cationic and neutral (σ-butenyl)nickel(II) complexes are examined,
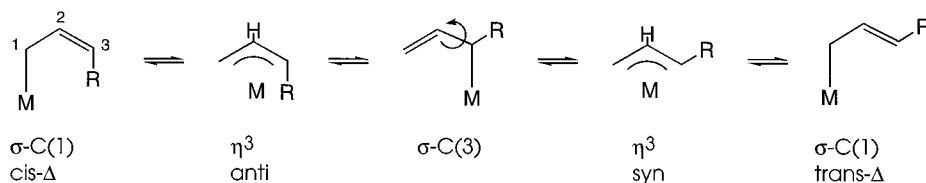
Figure 7. Different configurations and modes of coordination of the butenyl anion (R, organyl, f.i., the growing polybutadienyl chain).

with $L = PH_3$ and $X^- = I^-$, respectively, which allows an estimation of the barrier height of anti−syn isomerization. An anti−syn equilibrium has to be assumed for each of the butadiene π-complexes **3** and **4**, the insertion products **6a**, and the stable store complexes **2**, with the syn configuration having the thermodynamically more stable structure ($K_{a/s} \sim 10^1 - 10^2$).[5f,7a] Following the preferred *cis*-butadiene insertion (anti insertion), the isomerization of the actual *anti*-butenyl insertion product into the thermodynamically more stable and more reactive *syn*-butenyl form (note the anti−cis, syn−trans correlation) is required in order to proceed onto the most favorable reaction course, which yields a *trans*-1,4 polymer. Additionally, it is interesting to see whether the butadiene insertion or the anti−syn isomerization could be regarded as the rate-determining step in the polymerization cycle.

As indicated by experimental investigations, two different cases must be distinguished, the bis(triphenyl phosphite) complex $[Ni(\eta^3\text{-}C_3H_5)(P(OPh)_3)_2]PF_6$[7a] and the allylnickel iodide $[Ni(\eta^3\text{-}C_3H_5)I]_2$[18] complex, both of which are typical trans catalysts. For neutral ligand complexes, the thermodynamically more stable syn form immediately disappears with the addition of butadiene to the crotyl bis(triphenyl phosphite) starting complex, thus forming butenyl(monoligand)(butadiene) complexes, while the concentration of the anti form consequently increases.[7a] This presents evidence for the higher reactivity of the thermodynamically more stable syn form. Although the anti form only can be seen in the butadiene-containing reaction solution, practically no cis units are formed. Obviously, the *anti*-butenyl complex is not reactive, and the polymerization can proceed only after formation of the reactive syn form by anti−syn isomerization, which therefore must be considered as the rate-determining step in the catalytic cycle. Consequently, after all of the butadiene has been consumed, the syn form slowly appears again. By contrast, in the case of anionic ligand complexes, only the more reactive syn form can be seen by NMR spectroscopy.[19] Therefore, the anti−syn isomerization could be quite rapid, and the butadiene insertion must be considered as the rate-determining step.

The rate of anti−syn isomerization has been proven by experiment to be strongly dependent on the structure. In the bis(ligand) complexes **2**, the isomerization rate is very low ($k_{a/s} \sim 10^{-5}$ s^{-1}),[23] but in the butenyl-

(monoligand) complexes **3**, **4** and **6a**, the anti−syn isomerization can be considerably accelerated.[7] The low isomerization rate in **2** may be attributed to a 14-electron σ-complex formation, which is rather unfavorable by energy. On the other hand, a 18- to 16-electron shift occurs starting from the η^4-butadiene complexes **4**, giving rise to stable σ-structures, which should compete with the most favorable transition states of *cis*-butadiene insertion. Moreover, for the butenyl(monoligand) complexes, the co-coordination of a double bond from the growing chain or of butadiene seems to be possible, which should decrease the isomerization barrier by a considerable amount. The co-coordination should be nearly impracticable for **2**, as indicated by the crystal structure of $[Ni(\eta^3\text{-}C_4H_7)(P(OPh)_3)_2]PF_6$.[24] Therefore, the course of anti−syn isomerization will only be explored for the butenyl(monoligand) complexes.

The anti−syn isomerization in the η^3-coordinated butenyl group takes place via the formation of a NiC(3) σ-bond followed by rotation of the vinyl group around the C(2)−C(3) single bond[20] (cf. Figure 7). Since the rotation around a C−C single bond can be assumed to not have any significant kinetic barrier (if there is no steric hindrance), the isomerization barrier height could be estimated fairly well by the destabilization of the most stable σ-NiC(3) complex relative to the reactive butadiene complexes **4** or the insertion products **6a**, respectively. Furthermore, the formation of a NiC(1) σ-bond also gives rise to a free rotating C(2)−C(3) single bond, but in contrast to the σ-NiC(3) structure, the configuration of the butenyl group cannot be altered (cf. Figure 7). Therefore, stable σ-NiC(3) complexes are looked for, i.e., all structures discussed in this section are minima, having a positive Hessian eigenspectrum. The reported barrier heights for the anti−syn isomerization are estimated.

At this point, it is interesting to examine how the metal center may be coordinatively saturated in the process of η^3- to σ-NiC(3) butenyl group conversion in order to achieve a relatively low isomerization barrier. This may be possible if a double bond from the growing chain,[21] butadiene, or a counterion (which potentially should be able to occupy two coordination places such as $CF_3CO_2^-$, $B(O_2C_6H_4)_2^-$ [22]) can be coordinated additionally.

Four different types of σ-NiC(3) structures, as shown in Figure 8, are examined, those of which may stem from the insertion products, **6a**, as well as from the butadiene π-complexes, **3** and **4**. In **IS-A**, the double bond from the growing chain and butadiene in the η^2-mode are coordinated with Ni(II), thus forming a 16-

(18) (a) Harrod, J. F.; Wallace, L. R. *Macromolecules* **1969**, *2*, 449. (b) Matsumoto, T.; Furukawa, J. *J. Macromol. Sci., Chem.* **1972**, *A6*, 281. (c) Klepikova, V. I.; Kondratenkov, G. P.; Kormer, V.; Lobach, M. I.; Churlyaeva, L. A. *J. Polym. Sci., Polym. Lett.* **1973**, *11*, 193.

(19) (a) Warin, R. *J. Organomet. Chem.* **1980**, *185*, 413. (b) Kormer, V. A. *J. Polym. Sci., Polym. Lett.* **1976**, *14*, 317.

(20) Vrieze, K. Fluxional allyl complexes. In *Dynamic Nuclear Magnetic Resonance Spectroscopy*; Jackman, L. M., Cotton, F. A., Eds.; Academic Press: New York, 1975.

(21) Akermark, B.; Vitagliano, A. *Organometallics* **1985**, *4*, 1275.

(22) Wache, S. Ph.D. Thesis, University of Halle, Verlag Shaker, Aachen, Germany, 1993.

(23) (a) Gehrke, J.-P.; Taube, R.; Jahn, M.; Radeglia, R. *Z. Chem.* **1988**, *28*, 262. (b) Tolman, C. A. *J. Am. Chem. Soc.* **1970**, *92*, 6785.
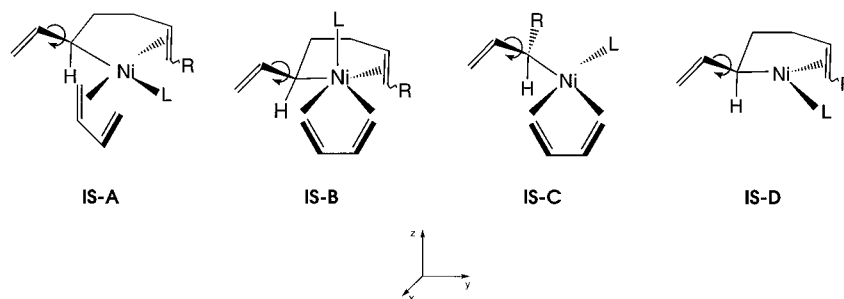
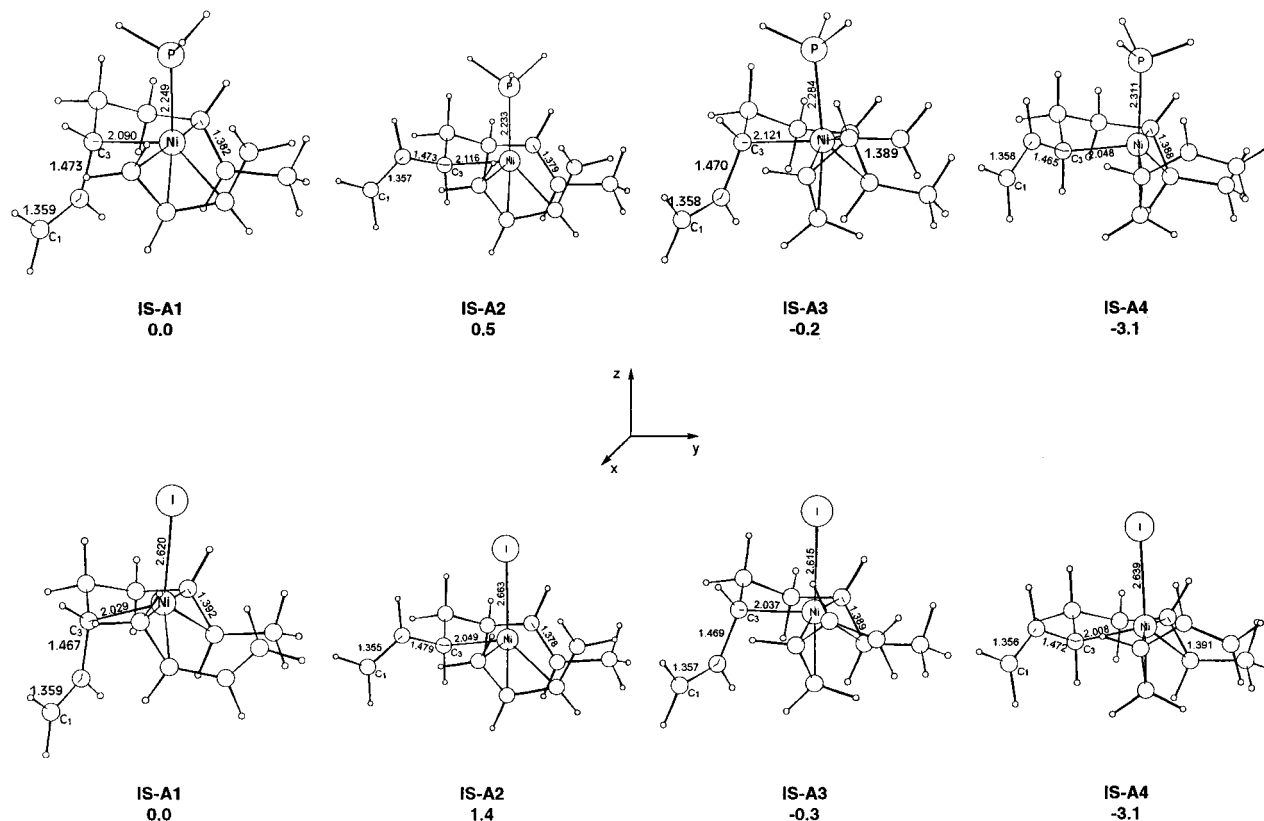**Figure 8.** Different types of stable σ-NiC(3) complexes (R, R′ = polybutadienyl chain).

Figure 9. Selected geometrical parameters of the optimized structures (Å) for the isomers of the most stable σ-NiC(3) complexes (L = PH$_3$ (top) and X$^-$ = I$^-$ (bottom)) together with the relative energies (ΔE in kcal/mol).

electron σ-complex, where the neutral or the anionic ligand lies within the quasi-planar coordination plane (assumed to be the xy plane). In the corresponding 18-electron η^4-butadiene structures **IS-B**, the neutral or the anionic ligand has to occupy an axial position similar to the butadiene complexes, **4**. Furthermore, 16-electron η^4-butadiene complexes **IS-C** can be formed, without participation of a double bond from the growing chain. By comparing the energetic behavior of these structures with the former ones, it should be possible to decide whether coordination of the double bond is required during the anti−syn isomerization. In addition, several types of 14-electron complexes can be formed, as shown in example **IS-D**. However, these structures should be energetically ruled out as stable σ-complexes describing a reasonable path for the isomerization.

The most stable σ-NiC(3) structures (**IS-A**, cf. Figure 8) stem from a 4-fold coordination of the metal center by σ-butenyl, η^2-*cis*-butadiene, the double bond from the growing chain, and the neutral ligand (L = PH$_3$) or the anionic ligand (X$^-$ = I$^-$). However, even after an

intensive search, no corresponding η^4-butadiene structures, **IS−B**, could be located in the case of anionic ligand coordination. Attempts to localize such structures immediately lead to the η^2-butadiene σ-NiC(3) complexes (**IS-A**). A quasi-η^4-butadiene coordination is possible concerning the neutral ligand, which is characterized by an elongated Ni−C bond opposite to the σ-butenyl due to the trans effect. However, butadiene is coordinated in an η^2-mode in the most stable σ-complex. The geometry of **IS-A** points at a quasi-tetrahedral coordination of the metal center. Four possible mutual orientations of the σ-NiC(3) butenyl group and η^2-butadiene in **IS-A** are shown in Figure 9 together with the relative energies with L = PH$_3$ and X$^-$ = I$^-$. In the most stable orientations, **IS-A1** (quasi-supine butadiene and the butenyl group which is directed toward below) and **IS-A4** (quasi-prone butadiene and the butenyl group which is directed toward above), both moieties can avoid best each other. The rather large Ni−C distance (greater than 2.3 Å) indicates only a weak coordinative interaction of the double bond from the growing chain with the metal center in the quasi-
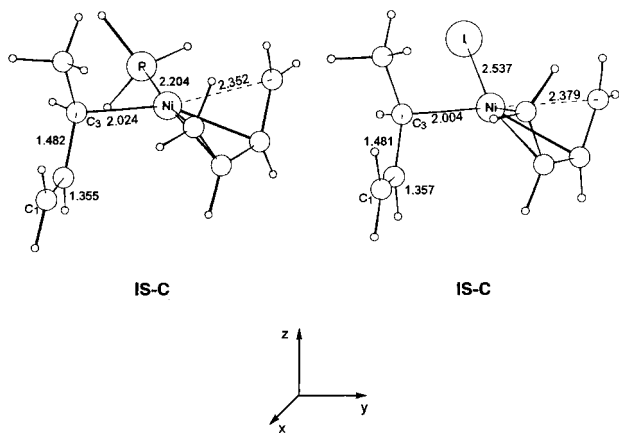
Figure 10. Selected geometrical parameters of optimized structures (Å) for the most stable isomer of IS−C (L = PH$_3$, right, and X$^-$ = I$^-$, left).

supine butadiene isomers (**IS-A1** and **IS-A2**). On the other hand, the quasi-prone butadiene isomers (**IS-A3** and **IS-A4**) are characterized by stronger double-bond coordination, which is comparable with the insertion products, **6a**. On the whole, for the neutral ligand, butadiene is quasi-η^4-coordinated, apart from the most stable **IS-A4** complex. In this case, butadiene is coordinated in an η^2-mode with a slightly enlarged Ni−ligand bond. The energetic gap between the η^4- and η^2-butadiene coordination modes amounts to 3.1 kcal/mol (ΔE). Butadiene is coordinated solely in an η^2-mode in neutral σ-complexes (where X$^-$ = I$^-$), which is caused by the greater donating ability of the anionic ligand. This should clearly favor η^2-coordination, since vinylethene can be a better π-acceptor than η^4-butadiene.

Thus, **IS-A4** represents the most stable σ-butenyl isomer regardless of whether neutral or anionic ligand are coordinated. Attempts to describe this complex by an open-shell triplet approach yields a total energy that is about 17 and 14 kcal/mol (ΔE) for L = PH$_3$ and X$^-$ = I$^-$, respectively, higher than in the closed-shell singlet case. The quasi-tetrahedral ligand coordination is obvious from the bonding angles ($\angle\sigma$-C(3)NiP ≈ 100/102°, $\angle$C(DB)[25] NiP ≈ 109/110°, $\angle$C(BD)[25] NiP ≈ 118/115°, for L = PH$_3$ and X$^-$ = I$^-$). For L = PH$_3$, the isomerization barrier can be evaluated to be about 13.0 kcal/mol with ZPC (13.2 kcal/mol using the Gibbs free energy) with respect to the anti form and to be about 15.8 kcal/mol with ZPC (16.1 kcal/mol using the Gibbs free energy) regarding the syn forms of the most stable η^4-butadiene complexes, **4-SS**. For X$^-$ = I$^-$, the barrier is about 10.2 and 13.1 kcal/mol with ZPC (10.7 and 13.4 kcal/mol using the Gibbs free energy), respectively.

The 16-electron η^4-butadiene complexes, **IS−C**, are essentially described by a quasi-planar coordination of the metal center. The most stable isomer is shown in Figure 10 for L = PH$_3$ and X$^-$ = I$^-$. In this case, the barrier height can be estimated to be about 28.3 kcal/mol (ΔE) with respect to the anti form and about 31.0 kcal/mol (ΔE) for the syn form of **4-SS**, for L = PH$_3$. For X$^-$ = I$^-$, the barrier was calculated to be about 14.2 and 17.3 kcal/mol, respectively.

Therefore, it can be concluded that structure **IS-A4** is the most stable σ-NiC(3) complex via which the anti−syn isomerization preferably proceeds. During this process, it seems to be essential to coordinatively saturate the metal center by co-coordination of butadiene and a double bond from the growing polymer chain or of the counterion. The isomerization barrier is decreased by about 3 kcal/mol by the anionic ligand as compared with the neutral ligand.
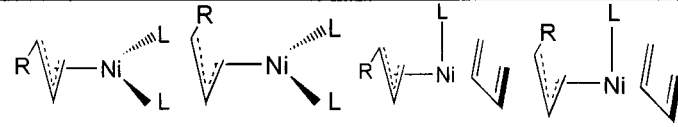
Unfortunately, from the stable σ-NiC(3) complexes, it is not possible to deduce the stage of the insertion process, i.e., from butadiene complexes **3** and **4** or the anti insertion product **6a**, from where the anti−syn isomerization may preferably take place. This would only be possible in a detailed "reaction path following" investigation, which was not done in this research. But this knowledge is not necessarily required if it can be assumed that all of the equilibria are being prepared under real polymerization conditions.

To evaluate which of the subsequent processes, insertion and anti−syn isomerization, will be the rate-determining step, the insertion barrier via the preferred reaction pathway has to be compared with the isomerization barrier. Obviously, in the case of anionic ligands, the *cis*-butadiene insertion is unfavored in energy by 3.1 kcal/mol with ZPC (3.2 kcal/mol by using the Gibbs free energy) relative to the isomerization. Therefore, the rate-determining step is the *cis*-butadiene insertion, which is in accord with the experiment. However, nearly identical barrier heights of both processes in the case of the neutral ligand (0.2 kcal/mol in favor of the isomerization with ZPC, 0.4 kcal/mol in favor of the insertion using the Gibbs free energy) may indicate that neither of them can be regarded as the rate-determining step. This is in contrast to experimental findings. We hope the extended modeling of organophosphorus ligands by PMe$_3$, P(OMe)$_3$, and PF$_3$, as given in the next section, will provide some further clarification on this topic.

Cationic [Ni(C$_4$H$_7$)L$_2$]$^+$ and [Ni(C$_4$H$_7$)(C$_4$H$_6$)L]$^+$ (L = PMe$_3$, P(OMe)$_3$, PF$_3$) Complexes. At this point, the effect of the different donor−acceptor ability of the neutral ligand on the thermodynamic and kinetic control of the *trans*-1,4-polymerization cycle will be investigated. To this end, the real *trans*-1,4-selective triphenyl phosphite and triphenylphosphine catalysts are modeled by P(OMe)$_3$ and PMe$_3$, respectively, rather than by the computationally less demanding but, regarding its chemical behavior, "improper" PH$_3$ (cf. preceding sections). Since the differences between PPh$_3$ and PMe$_3$ are small compared with the differences with PH$_3$, as found by Schmid[26a] and Häberlein[26b] for bond dissociation energies and for structural parameter as well, we also expect to find minor differences between P(OPh)$_3$ and P(OMe)$_3$. In addition, PF$_3$ served as a possible model ligand. Therefore, a broad range of the neutral ligand's basicity can be modeled, which should decrease in the order PMe$_3$ > P(OMe)$_3$ > PF$_3$.
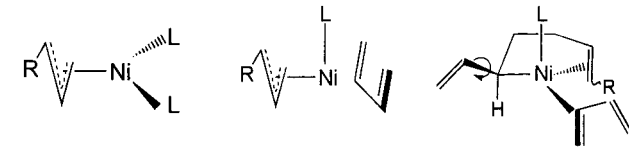
First the thermodynamic control is examined, followed by an evaluation of the kinetic control, including the anti−syn isomerization. Bearing in mind the

(24) Kempe, R.; Sieler, J.; Wache, S.; Taube, R. *Z. Kristallographie* **1993**, *207*, 249.
(25) S(DB) stands for the center of the double bond in the growing chain. S(BD) stands for the center of η^2-coordinated butadiene.

(26) (a) Schmid, A.; Herrmann, W. A.; Frenking, G. *Organometallics* **1997**, *16*, 701. (b) Häberlein, O. D.; Rösch, N. *J. Phys. Chem.* **1993**, *97*, 4970. (c) Jacobsen, H.; Berke, H. *Chem. Eur. J.* **1997**, *3*, 881.

Table 5. Calculated Potential-Energy (with and without ZPC) and Gibbs Free-Energy Differences between Cationic Bis(ligand) $[Ni(\eta^3\text{-}C_4H_7)L_2]^+$ and η^4-Butadiene $[Ni(\eta^3\text{-}C_4H_7)(C_4H_6)L]^+$ Complexes (kcal/mol)^{a,b}

L	2s	2a	4s-SS	4a-SS
PMe₃	0.0 (0.0) *0.0*	-0.3 (-0.5) *-0.9*	8.3 (8.8) *10.3*	12.9 (13.5) *15.2*
P(OMe)₃	0.0 (0.0) *0.0*	-0.7 (-0.6) *-1.0*	7.2 (8.2) *8.5*	10.0 (11.4) *12.9*
PH₃	0.0 (0.0) *0.0*	1.3 (1.3) *1.1*	-1.9 (-1.8) *1.6*	0.9 (1.0) *4.5*
PF₃	0.0 (0.0) *0.0*	0.8 (1.0) *2.5*	-19.6 (-18.3) *-15.4*	-16.8 (-15.5) *-12.1*

^{a} The most stable store complex **2s** was chosen as the energetic reference in each case. ^{b} Numbers in parentheses include the zero-point correction while those in italics are the Gibbs free energies.

Table 6. Natural Net Charges on Nickel and on the Ligand (in Italic)[27]

L	2s^a	4s-SS	IS-A4
PMe₃	0.385 / *0.379*	0.699 / *0.382*	0.743 / *0.294*
P(OMe)₃	0.314 / *0.382*	0.662 / *0.338*	0.705 / *0.268*
PH₃	0.394 / *0.322*	0.686 / *0.296*	0.728 / *0.233*
PF₃	0.227 / *0.340*	0.585 / *0.265*	0.625 / *0.205*
I⁻	0.522 / *-0.322*	0.755 / *-0.508*	0.791 / *-0.527*

^{a} Averaged values for ligand net charges.

present computational resources available, the calculations are restricted to full optimizations of only the key structures located in the case of L = PH₃ by simply replacing PH₃ by PMe₃, P(OMe)₃, and PF₃. These are **2** and **4**-*SS* for the thermodynamic control, **5**-*PP* for the kinetic control, and **A4** for anti−syn isomerization. Since the structural features of the complexes are rather similar by changing the ligand, they are not depicted (but contained in the Supporting Information) and only the energetic and electronic properties are discussed in detail.

The different ligand basicity significantly influences the position of the ligand substitution equilibrium (cf. Table 5). In contrast to the roughly similar energetic gap between the anti and syn forms by varying the ligand, the bis(ligand) complex, **2s**, is stabilized by 8.8 and 8.2 kcal/mol with ZPC (10.3 and 8.5 kcal/mol using the Gibbs free energy) with respect to the butadiene complex **4s**-*SS* with L = PMe₃ and P(OMe)₃, respectively. In the case of L = PF₃, **2s** is by about 18.3 kcal/mol, with ZPC (15.4 kcal/mol using the Gibbs free energy), less stable than **4s**-*SS*. Therefore, as compared with PH₃, increasing the ligand's nucleophily (L = PMe₃, P(OMe)₃) shifts the equilibrium position largely onto the side of the bis(ligand) complexes whereas decreasing the ligand's nucleophily (L = PF₃) shifts the equilibrium position still further on the side of the butadiene complexes. For the more reliable PMe₃ and P(OMe)₃ model ligands, **2** seems to be too stable with respect to **4** as one can deduce from experimental findings. How-

ever, it is worthwhile to note that the equilibrium position's shift toward **2** shows up in the right direction upon going from PH₃ to PMe₃ and P(OMe)₃, leaving the steric influence to a great extent disregarded. The main reason for the insufficient description by using PH₃ comes from the improper description of the real ligand's basicity.

An indication of the different ligand's donating ability is given by the natural net charges[27] of nickel and the ligands (cf. Table 6). The electron density of nickel is essentially determined by its acceptor strength, which should increase with the decreasing of the ligand's donor strength. Therefore, for the calculated metal charges, the ligand's basicity decreases in the order PMe₃ ≈ PH₃ > P(OMe)₃ ≫ PF₃. Although the general trend is correct, the discrepancy between the derived ligand's basicity and the equilibrium position for PH₃ is obvious. This is mainly caused by the general inadequacy of most types of population analyses to reliably describe transition metal charges. A better description is given by the ligand's charges (cf. Table 6), which gives rise to a PMe₃ ≈ P(OMe)₃ > PH₃ > PF₃ ranking of the decreasing ligand's basicity, which is in much better accord with the derived equilibrium position.

Moreover, the different ligand's basicity also influences the barrier height for butadiene insertion and anti−syn isomerization (cf. Table 7). The butadiene

(27) Reed, A. E.; Curtiss, L. A.; Weinhold, F. *Chem. Rev.* **1988**, *88*, 899.

Table 7. Calculated Potential-Energy (with and without ZPC) and Gibbs Free-Energy Barriers for
***cis*-Butadiene Insertion As Compared with *Anti−Syn* Isomerization Concerning Cationic**
Butenyl(monoligand) Complexes [Ni(η^3-RC$_3$H$_4$)L]$^+$ (kcal/mol)^{a,b}

L	5s-PP	5a-PP	IS-A4
PMe$_3$	16.4 (16.4) *16.8*	19.3 (19.2) *19.3*	19.2 (18.3) *17.9*
P(OMe)$_3$	14.8 (15.2) *16.2*	18.4 (18.8) *19.8*	18.1 (17.6) *18.0*
PH$_3$	16.2 (16.0) *15.7*	20.5 (20.6) *20.5*	16.5 (15.8) *16.1*
PF$_3$	15.2 (14.9) *15.5*	19.8 (19.9) *20.4*	16.1 (15.2) *15.5*

^{a} The most stable butadiene complex **4s**-*SS* was chosen as the energetic reference in each case. ^{b} Numbers in parentheses include the zero-point correction while those in italics are the Gibbs free energies.

insertion via the most stable anti and syn transition states is effected by the different ligand's nucleophily to only a small degree. Compared with PH$_3$, it amounts to about ±1 kcal/mol for the syn form. On the other hand, the higher basicity of the PMe$_3$ and P(OMe)$_3$ model ligands increases the isomerization barrier by about 2.5 and 1.8 kcal/mol, with ZPC (1.8 and 1.9 kcal/mol using the Gibbs free energy), with respect to PH$_3$. This may be attributed to an increasing donating effect of the butenyl group toward the metal center when going from the η^3-π to the η^1-σ coordination. Therefore, the formation of stable Ni−C(3) σ-complexes should be hampered by increasing the ligand's donating ability. As a consequence, the energetic gap between the structures that describe butadiene insertion and isomerization is increased by increasing the ligand's basicity. The rate-determining step is the anti−syn isomerization, which is unfavored by about 1.9 and 2.4 kcal/mol with ZPC (1.1 and 1.8 kcal/mol using the Gibbs free energy) relative to butadiene insertion for L = PMe$_3$ and P(OMe)$_3$, respectively. On the other hand, the energetic gap is not noticeably influenced by reducing the ligand's donating ability upon going from PH$_3$ to PF$_3$.

To conclude, a reliable modeling of the organophosphorus ligand's basicity is necessary to achieve a well-balanced description of both the thermodynamic and kinetic control of the *trans*-1,4 polymerization of butadiene. At least PMe$_3$ and P(OMe)$_3$ have to serve as a model for PPh$_3$ and P(OPh)$_3$ as far as relative energies are concerned. The often used parent system PH$_3$ is clearly improper for this purpose. We agree with Schmid et al.[26a] and Jacobsen et al.[26c] who may point to the fact that one has to be extremely careful when using PH$_3$ as a computationally less demanding and simplified model of catalyst-relevant organophosphines.

Final Gibbs Free-Energy Profile. The final Gibbs free-energy profiles of the entire catalytic cycle of the 1,4-polymerization of butadiene with cationic butenylbis(ligand) complexes [Ni(η^3-RC$_3$H$_4$)L$_2$]$^+$ (L = PH$_3$, P(OMe)$_3$) and neutral dimeric butenyl complexes [Ni(η^3-RC$_3$H$_4$)X]$_2$, (X$^−$ = I$^−$), as the catalyst are given in Schemes 2 and 3, respectively.

In addition to the features which were discussed in detail in the previous sections the following observations are worth noting. First, regardless of whether η^2- or η^4-coordination occur, butadiene is capable of replacing the last π-coordinated double bond of the growing chain. Therefore, due to the formation of reactive butenyl-(monoligand)(butadiene) complexes **4s**, the chain propagation can proceed. Second, for the neutral dimeric butenyl complexes, the anion bridge is destroyed by butadiene coordination. Third, for the cationic complexes, the calculated insertion barrier (for L = (P(OMe)$_3$) corresponds remarkably with the value determined by experiment (for L = P(OPh)$_3$), which amounts to 20.3 kcal/mol[7e,28] relative to the most stable store complex under polymerization conditions.

Conclusions

The energetic profile of the entire catalytic cycle of the 1,4-polymerization of butadiene was theoretically calculated by applying the density functional theory with cationic butenylbis(ligand) [Ni(η^3-RC$_3$H$_4$)L$_2$]$^+$ complexes (summarized in Scheme 2) and neutral dimeric butenyl [Ni(η^3-RC$_3$H$_4$)X]$_2$ (summarized in Scheme 3) complexes as the catalyst. Geometry optimization of the intermediates and transition states involved in each step of the catalytic cycle according to the π-allyl-insertion mechanism proposed by Taube et al. was performed for almost all isomers. We believe that this is the first comprehensive theoretical study that deals with the stereoselective polymerization of butadiene by means of reliable nonempirical methods.

The investigations were carried out on different model systems of the catalytically active butenyl(monoligand)-(butadiene)nickel(II) complexes [RC$_3$H$_4$Ni(C$_4$H$_6$)L]$^+$, and [RC$_3$H$_4$Ni(C$_4$H$_6$)X], and [Ni(C$_4$H$_7$)(C$_4$H$_6$)L]$^+$ with L = C$_2$H$_4$, PH$_3$ and [Ni(C$_4$H$_7$)(C$_4$H$_6$)X] with X$^−$ = I$^−$. In addition, to examine the reliability of modeling organophosphorus ligands by the simplified PH$_3$ ligand, L = PMe$_3$, P(OMe)$_3$, and PF$_3$ were examined. On the basis

(28) *Homogene Katalyse*, Taube, R., Ed.; Akademie-Verlag: Berlin, Germany, 1988.

Scheme 2. Gibbs Free-Energy Profile (kcal/mol) of the Entire Catalytic Cycle of the 1,4-Polymerization of Butadiene with Cationic Butenylbis(ligand) Complexes [Ni(η^3-RC$_3$H$_4$)L$_2$]$^{+a}$ as the Catalyst
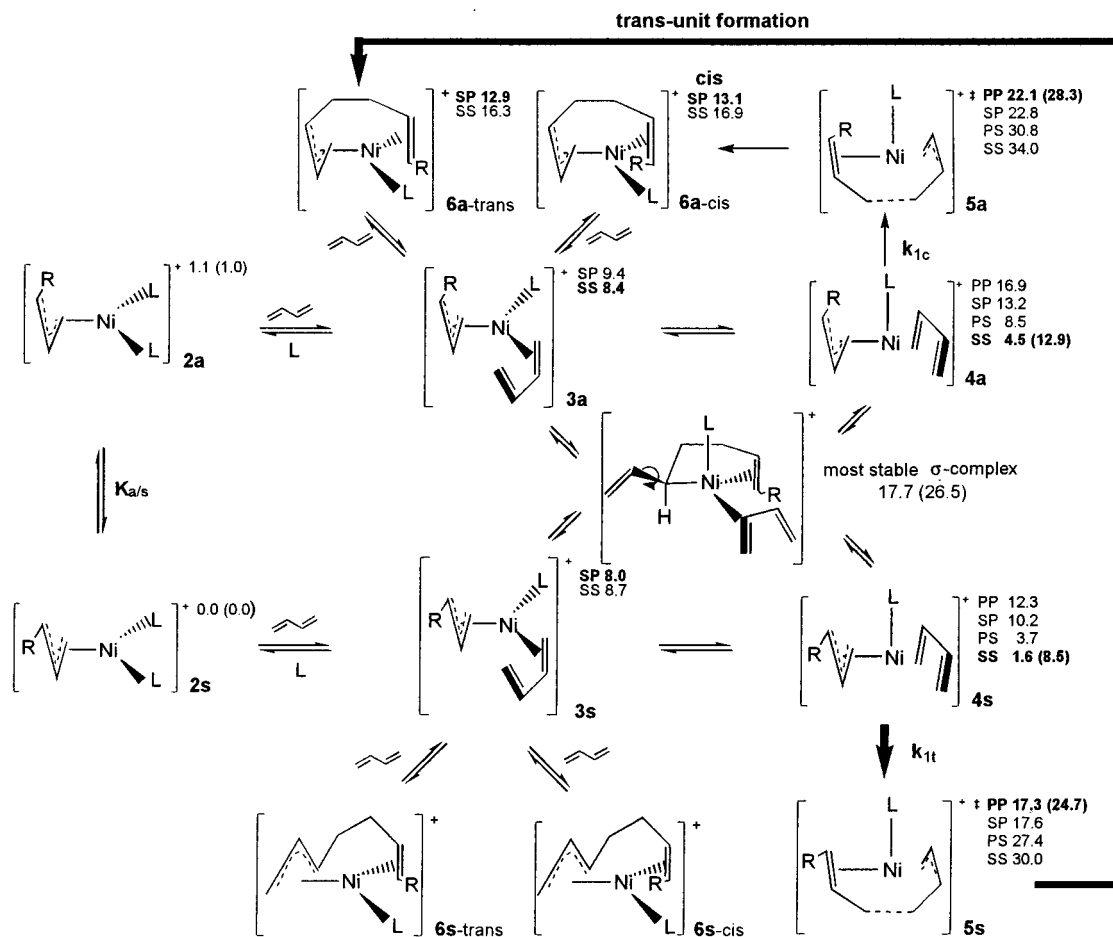
^{a} L = PH$_3$, P(OMe)$_3$ (in parentheses). Different isomers of a given species are distinguished (for abbreviations see text), with the most stable isomer marked bold.

of the supposed π-allyl-insertion mechanism, which is supported in all essential features of this research, the calculations clearly indicate an understanding of the kinetic and thermodynamic control of catalytic activity and cis–trans selectivity as well as elucidate the mechanism of stereoregulation.
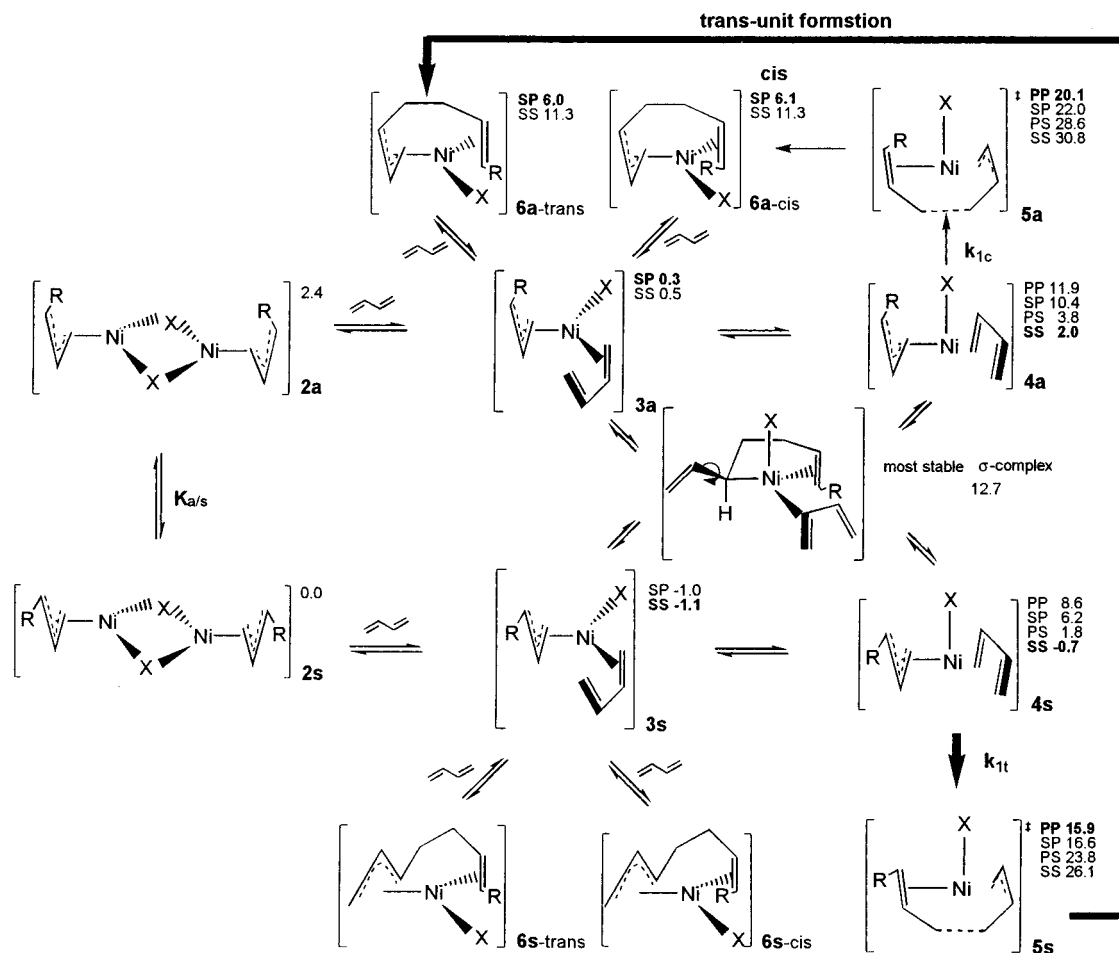
The following key conclusions may be drawn from the calculations presented here. (1) The insertion of butadiene into the butenylnickel(II) bond starts solely from the single cis configuration of butadiene, irrespective of the mode of its coordination. It can take place within the π-coordination of the butenyl group and butadiene while maintaining the π-interaction of the reactive parts with the metal center in the course of the whole reaction. Simultaneously with the C–C bond formation, from the butadiene an η^3-coordinated butenyl group in the anti configuration is regenerated as the chain end, thus allowing the polymerization to proceed.

(2) Coordination of a double bond from the growing polymer chain or of an additional neutral or anionic ligand is necessary in order to make the insertion thermodynamically possible and kinetically feasible, in compliance with Tolman's 18–16-electron rule. A clear difference in the stability and reactivity of butenyl-(monoligand)(butadiene)nickel complexes, with regard to the mutual orientation of butenyl and butadiene, is caused by an additional ligand. They are best observed in the transition states, i.e., supine butadiene gives rise

to product-like tetragonal pyramidal and prone butadiene leads to educt-like trigonal bipyramidal transition states. The transition states are characterized by an almost complete change in the hybridization of the affected carbon atoms of the newly formed C–C σ-bond from sp^2 to sp^3.

(3) The stability and reactivity of the different isomers of the butadiene complexes, **4**, is calculated to be very similar and quite comparable, regardless of the donor–acceptor ability of the neutral or the anionic ligand. In each case, the syn forms are more stable than the anti counterparts and η^4-coordination is preferred, in general, to η^2-butadiene coordination. The stability of the different isomers of **4** is mainly determined by the kind of butadiene orientation rather than that of the butenyl group, which is less pronounced. The most stable isomers of **4** stem from the *syn-SS* coordination, whereas the most stable *syn-SP* η^2-butadiene complexes are disfavored by 1.7, 6.0, and 8.5 kcal/mol (ΔE) for I$^-$, C$_2$H$_4$, and PH$_3$, respectively. This gap becomes considerably decreased by the stronger donating anionic ligand, since the η^2-coordination can compete better with the η^4-coordination with increasing electron density on the metal center.

(4) The thermodynamically more stable *syn*-butenyl forms are also more reactive than the corresponding anti counterparts. Prone butadiene isomers of **4** are calculated to be much more reactive than the corresponding

Scheme 3. Gibbs Free-Energy Profile (kcal/mol) of the Entire Catalytic Cycle of the 1,4-Polymerization of Butadiene with Neutral Dimeric Butenyl Complexes [Ni(η^3-RC$_3$H$_4$)X]$_2$[a] as the Catalyst

trans-unit formation

| 6a-trans | SP 6.0, SS 11.3 | 6a-cis | cis, SP 6.1, SS 11.3 | 5a | ‡ PP 20.1, SP 22.0, PS 28.6, SS 30.8 |

2a : 2.4 ... 3a : SP 0.3, SS 0.5 ... 4a : PP 11.9, SP 10.4, PS 3.8, **SS 2.0**

most stable σ-complex 12.7

2s : 0.0 ... 3s : SP -1.0, **SS -1.1** ... 4s : PP 8.6, SP 6.2, PS 1.8, **SS -0.7**

6s-trans ... 6s-cis ... 5s : ‡ PP 15.9, SP 16.6, PS 23.8, SS 26.1

K$_{a/s}$ k$_{1c}$ k$_{1t}$

[a] X$^-$ = I$^-$. Different isomers of a given species are distinguished (for abbreviations see text), with the most stable isomer marked bold.

supine forms. For the most stable *SS* orientation, the insertion is disabled by a rather large barrier, and, therefore, the reactive butadiene and butenyl moieties must change their mutual orientation in order to open the most favorable pathway via prone butadiene transition states. Although both kinds of butadiene complexes should be in comparable concentrations in the educt equilibrium, the η^2-butadiene π-complexes cannot be considered as the direct precursors of the transition states for butadiene insertion. Due to the similar kind of butadiene coordination, the transition states must be formed via the η^4-butadiene π-complexes, in accord with the principle of least-structure variation. Therefore, the η^2-butadiene complexes could be regarded as possible starting but transient π-complexes during the process of forming the η^4-butadiene complexes.

(5) Nearly identical activation barriers for the *anti*- and *syn*-butenyl forms indicate a similar intrinsic reactivity, regardless of the butenyl group's configuration. The intrinsic reactivity becomes diminished with increasing the ligand's donating ability in the order C$_2$H$_4$ > PH$_3$ > I$^-$, as indicated by the activation barrier's growth (including ZPC) of each of about 2 kcal/mol in the order C$_2$H$_4$ (2.6 kcal/mol), PH$_3$ (4.5 kcal/mol), and I$^-$ (6.4 kcal/mol) for the most reactive butadiene complexes. Under purely kinetic control, *cis*-butadiene insertion would preferably proceed via *syn*-butenyl

prone butadiene transition states, regardless of whether *SP* or *PP* orientations are concerned, thus opening the *trans*-1,4 reaction channel, which yields a polymer product that in turn does not possess any stereoselectivity in the methylene groups. The participation of the double bond from the growing polymer chain is not required in this process. Alternative pathways, i.e., via *anti*-butenyl prone butadiene transition states, forming a *cis*-1,4 polymer, or the direct generation of *trans*-1,4 products by inserting *trans*-butadiene, are strongly unfavored by higher kinetic barriers.

(6) The chain propagation by the formation of *trans*-1,4-polymer units can, however, only take place if butadiene is capable of replacing the last π-coordinated double bond of the growing polymer chain, thus forming a new reactive butenyl(monoligand)(butadiene) complex. The calculations show a clear indication in this direction. On the other hand, butadiene should not be capable of substituting the neutral or the anionic ligand, thus forming ligand-free butenyl(butadiene)nickel complexes, which should catalyze the formation of *cis*-1,4 units. In experiment, a *cis*-selectivity of at least of 5% of the typical trans catalysts[5c,d] (which corresponds to a difference between the transition states of about 1.8 kcal/mol) was observed. Due to the intrinsic *trans*-selectivity of cationic or neutral butenyl(monoligand)-nickel complexes, this remaining *cis*-selectivity can only

be elucidated if under thermodynamic control, as a result of a subsequent ligand butadiene substitution, the *cis*-1,4 channel may be opened by ligand-free butenyl(butadiene)nickel complexes.

(7) To achieve a well-balanced description of both the thermodynamic and kinetic control of the *trans*-1,4-polymerization of butadiene, a reliable modeling of the organophosphorus ligand's basicity (besides steric effects) is necessary. At least PMe_3 and $P(OMe)_3$ have to serve as models for PPh_3 and $P(OPh)_3$ as far as relative energies are concerned. One has to be extremely careful in using PH_3 as a computationally less demanding and simplified model of catalyst-relevant organophosphines.

(8) The anti−syn isomerization takes place in a tetrahedrally coordinated σ-NiC(3) complex, where butadiene is bound in an η^2-mode. The participation of the double bond from the growing polymer chain and/or an additional ligand or counterion is demanded in this process.

(9) The position of the substitution equilibrium was estimated to be shifted greatly onto the side of the bis-(ligand) complexes with the increasing neutral ligand's basicity and in the opposite direction if its nucleophily decreases.

(10) On the basis of thermodynamic and kinetic control, important differences in the reaction mechanism for neutral and anionic ligands appear. The equilibrium constant for the process of forming the real catalyst complexes, **4**, is larger for anionic ligands compared with neutral ligands. This relation is the opposite for the rate constant of the insertion process. Therefore, the catalytic activity of cationic butenyl-(monoligand) complexes should be determined mainly by the concentration of the active butadiene complexes rather than by their reactivity. As a consequence, the catalytic activity is thermodynamically controlled for the most part in this case, similar to the cis−trans selectivity. By contrast, the catalytic activity on the whole is kinetically controlled in the case of neutral butenyl-(monoligand) complexes. As indicated by experimental findings, neutral ligand systems are slightly more reactive than anionic ligand systems.

(11) The following conclusions may be drawn by comparing the barrier calculated for *cis*-butadiene insertion and anti−syn isomerization: The rate-determining step is the *cis*-butadiene insertion for the neutral complexes (where $X^- = I^-$) and the anti−syn isomerization for the cationic complexes (where $L = PMe_3$, $P(OMe)_3$), both of which are in accordance with the experiment. Additionally, one has to consider that the balance of both processes may also be influenced by steric reasons. With the increasing of the ligand's bulkiness, the formation of stable σ-NiC(3) complexes should be hampered to a greater extent than the formation of the transition states of insertion. The participation of a double bond from the growing chain is demanded in the first process but not in the second process. Therefore, based on purely steric grounds, the anti−syn isomerization could be disfavored versus butadiene insertion for bulky neutral ligands like $P(OPh)_3$.

It should be mentioned that the nickel-catalyzed 1,4-polymerization is energetically favored relative to the 1,2-polymerization, which originates from a C(1)−C(3) connection of the butadiene and butenyl moieties. This will be studied in detail in a forthcoming paper.

Supporting Information Available: Tables of Cartesian coordinates of selected optimized structures (7 pages). Ordering information is given on any current masthead page.

OM9705923